## TECHNICAL REPORT STANDARD PAGE

| 1. Report No. | 2. Government Accession No. | 3. Recipient's Catalog No. |
|---|---|---|
| **FHWA/LA.09/444** | | |

| 4. Title and Subtitle | 5. Report Date |
|---|---|
| **Analysis of Seasonal Strain Measurements in Asphalt Materials under Accelerated Pavement Testing and Comparing Field Performance and Laboratory Measured Binder Tension Properties** | **June 2009** |
| | 6. Performing Organization Code<br>**LTRC** |
| 7. Author(s)<br>**Mostafa A. Elseifi, Ph.D.** | 8. Performing Organization Report No.<br>**LTRC Project No. 08-2P**<br>**State Project No. 736-99-1519** |
| 9. Performing Organization Name and Address<br>**Louisiana State University**<br>**Department of Civil and Environmental Engineering**<br>**3508 Patrick Taylor Hall**<br>**Baton Rouge, LA 70803** | 10. Work Unit No.<br><br>11. Contract or Grant No. |
| 12. Sponsoring Agency Name and Address<br>**Louisiana Transportation Research Center**<br>**4101 Gourrier Avenue**<br>**Baton Rouge, LA 70808** | 13. Type of Report and Period Covered<br>**Final Report**<br>**2008**<br>14. Sponsoring Agency Code<br>**LTRC** |

15. Supplementary Notes

**Conducted in cooperation with the U.S. Department of Transportation, Federal Highway Administration**

16. Abstract

Seasonal variation of measured pavement responses with temperature and its relationship to pavement performance has not been thoroughly evaluated for ALF Experiments II and III. Such information may be used to improve instrumentation strategies in future ALF experiments. These results may also be used to establish the relationship between binder elongation properties at intermediate and low temperature and mix performance. Such link may be used to update current binder standards by specifying measurement of properties that are indicative of pavement performance. Such properties may be obtained by complementing or modifying current specifications with the direct tensile test or the multiple stress creep recovery test instead of the current ductility test. The objectives of this study were two fold. First, instrument responses in past ALF Experiments were analyzed to quantify the impacts of seasonal variation of pavement responses with temperature and its relationship to pavement performance. Second, nine straight asphalt binders obtained from two asphalt suppliers were tested to link laboratory measured properties to mix performance. Based on the results of this analysis, it is concluded that survivability and repeatability of the gages were acceptable in past experiments. However, strain gages were not a reliable indicator of damage development in hot-mix asphalt (HMA). Laboratory test results showed that a binder that provides high ductility at intermediate temperature would be characterized by poor elongation properties at low temperature. This trend was related to the binder fractional compositions as an increase in the binder content of low molecular weight results in an increase in its ductility at intermediate temperature. However, an increase in paraffinic maltene content results in the binder tending to crystallize at higher temperature as it approaches the glassy region. Based on the results of laboratory testing conducted in this study, it is recommended that the ductility test be kept in the state binder's specifications as it correlates well with mix performance at intermediate temperature. This test may not be substituted with the direct tensile test or the multiple stress creep recovery test.

| 17. Key Words | 18. Distribution Statement |
|---|---|
| Accelerated Pavement testing, Instrumentation, Ductility, Direct Tensile Test | Unrestricted. This document is available through the National Technical Information Service, Springfield, VA 21161. |

| 19. Security Classif. (of this report) | 20. Security Classif. (of this page) | 21. No. of Pages | 22. Price |
|---|---|---|---|
| N/A | None | 86 | N/A |

## Project Review Committee

Each research project has an advisory committee appointed by the LTRC director. The Project Review Committee (PRC) is responsible for assisting the LTRC administrator or manager in the development of acceptable research problem statements, requests for proposals, review of research proposals, oversight of approved research projects, and implementation of findings.

LTRC appreciates the dedication of the following Project Review Committee members in guiding this research study to fruition.

### LTRC Administrator/Manager

Zhongjie "Doc" Zhang, Ph.D., P.E.
Pavement and Geotechnical Research Administrator

### Members

Chris Abadie
Phil Arena
Steve Cumbaa
Jason Davis
Mohammad Khattak
Louay Mohammad
Hak Shul
Zhong Wu

### Directorate Implementation Sponsor

William Temple, P.E.
DOTD Chief Engineer

# Analysis of Seasonal Strain Measurements in Asphalt Materials under Accelerated Pavement Testing and Comparing Field Performance and Laboratory Measured Binder Tension Properties

by

Mostafa A. Elseifi, Ph.D.
Assistant Professor
Department of Civil and Environmental Engineering
Louisiana State University
3506 Patrick Taylor Hall, Baton Rouge, LA 70803
e-mail: elseifi@lsu.edu

LTRC Project No. 08-2P
State Project No. 736-99-1519

conducted for

Louisiana Department of Transportation and Development
Louisiana Transportation Research Center



June 2009

# ABSTRACT

Quantitative performance of lane test sections at the accelerated loading facility (ALF) facility has been successfully established in terms of evolution of rutting and cracking with the number of repetitions. In addition, instruments' responses were used to provide an indication of the performance of the different test sections and to validate developed theoretical models. However, seasonal variation of measured pavement responses with temperature and its relationship to the predicted performance has not been thoroughly evaluated for ALF Experiments II and III. Such information may be used to improve instrumentation strategies in future ALF experiments. Results of past ALF experiments may also be used to link laboratory measured properties of asphalt binders to the mixture performance. Such a link may be used to update current binder standards by specifying measurements of properties that are indicative of pavement performance. Such properties may be obtained by complementing or modifying current specifications with the direct tensile test (DTT) or a newly-developed dynamic shear rheometer (DSR) test (i.e., the multiple stress creep recovery test) instead of the current ductility test.

Instrument responses in past ALF experiments were analyzed to quantify the impacts of seasonal variation of pavement responses with temperature and its relationship to pavement performance. In addition, nine straight asphalt binders obtained from two asphalt suppliers were tested to link laboratory measured properties to mix performance. Based on the results of this analysis, it is concluded that survivability and repeatability of the gages were acceptable in past experiments. However, installed pressure cells in the granular layers appeared to tilt during construction or after the loading started possibly due to poor compaction of the supportive layer. In addition, strain gages were not a reliable indicator of damage development in hot-mix asphalt (HMA). It appears that with the increase in number of passes, strain gages disperse the material around them resulting in less contact with the surrounding medium and therefore, a smaller strain was measured. Measured vertical stress remained fairly constant with the increase in number of passes. This observation indicates that the stress applied on the material mainly depends on the magnitude of the external load and not on the level of damage in the material.

Laboratory test results showed that a binder that provides high ductility at intermediate temperature would be characterized by poor elongation properties at low temperature. This trend was related to the binder fractional compositions as an increase in the binder content of low molecular weight (LMW) results in an increase in its ductility at intermediate temperature. However, an increase in paraffinic maltene content results in the binder tending to crystallize at higher temperature as it approaches the glassy region. Based on the results

of laboratory testing conducted in this study, it is recommended that the ductility test be kept in the state binder's specifications as it correlates well with mix performance at intermediate temperature. This test may not be substituted with the direct tensile test or the multiple stress creep recovery test.

# ACKNOWLEDGMENTS

The author recognizes the efforts of Dr. Louay Mohammad, Chris Abadie, Dr. Zhongjie Zhang, Dr. Ionela Glover, Dr. Ioan Negulescu, and Dr. William H. Daly who cooperated with the research team during this project. This was critical for conducting, assessing, and interpreting the laboratory results obtained in this study. The author would also like to acknowledge the assistance of Terry Naidoo, Seth Bradley, Wanggan Yang, and Matt Davis of Louisiana State University.

The U.S. Department of Transportation (USDOT), Federal Highway Administration (FHWA), Louisiana Department of Transportation and Development (LADOTD), and Louisiana Transportation Research Center (LTRC) financially supported this research project. The assistance of the asphalt laboratory staff at LTRC is greatly appreciated. Per LTRC's request, The International System of Units (SI) is used in the binder section of this report and English units are used in the instrumentation section of this report.

# IMPLEMENTATION STATEMENT

A detailed instrumentation plan for future ALF experiments is provided as a result of this research project. This plan calls for a number of modifications to past instrumentation strategies. This includes intensifying measurements in the early stage of the experiment, using temperature sensors such as thermocouples, increasing the distance between the sensors in the longitudinal direction, and improving the compaction of pressure gages. In addition, the use of cement-stabilized materials at the ALF facility needs to be investigated since it extends the experiment over a long period of time that may not be necessary. The benefits of this layer are well established for the state of Louisiana. However, since most of the research conducted at the ALF facility is related to the upper HMA layers, avoiding cement-treated materials in future ALF experiments may permit the assessment of the relative performance of different pavement technologies in a cost and time-effective manner.

Measurement of binder ductility is beneficial to the state and correlates well with mix performance at intermediate temperatures. This test may not be substituted with the direct tensile test or the multiple stress creep recovery test. It is recommended that the ductility test be kept in the state binder's specifications.

# TABLE OF CONTENTS

# LIST OF TABLES

# LIST OF FIGURES

# INTRODUCTION

Since 1996, the LADOTD has utilized LTRC's ALF at the Pavement Research Facility to determine the effectiveness of innovative pavement technologies in an environment that closely resembles actual in-service field conditions. In Experiment I, conventional and alternative base materials were evaluated. In Experiment II, benefits of using powdered rubber in HMA surfaces and base course mixes were quantified and validated. In Experiment III, the use of reclaimed asphalt pavement (RAP) base layers was investigated instead of conventional base course asphalt mixes. In Experiment IV, the use of blended calcium sulfate base and foamed asphalt recycled base was evaluated as compared to conventional base course asphalt mixes.

In these past experiments, quantitative performance of the test lanes was established in terms of evolution of rutting and cracking with the number of repetitions. In addition, instrument responses were used to provide an indication of the performance of the different test sections and to validate developed theoretical models. In these experiments, a wide array of sensors was used, including H-type strain gage and earth pressure cells. However, the seasonal variation of measured pavement responses with temperature and its relationship to the predicted performance has not been thoroughly evaluated for ALF experiments. Such information may be used to improve instrumentation strategies in future ALF experiments and to determine the evolution of damage with the increase in the number of repetitions.

Results of past ALF experiments may also be used to link laboratory measured properties of asphalt binders to the measured performance of hot-mix asphalt. Such a link may be used to update current binder standards by specifying measurements of properties that are indicative of pavement performance. Such properties may be obtained by complementing or modifying current specifications with the direct tensile test (DTT) or a newly-developed dynamic shear rheometer (DSR) test (i.e., multiple stress recovery creep test) instead of the current ductility test. This test has been used in Louisiana as a specification for straight asphalt binder, but a number of asphalt suppliers from out of state indicated that their products only comply with the Superpave binder specification system as it is required by many states without considering conventional tests, such as the ductility test.

## Literature Review

### Accelerated-Pavement Testing

Accelerated-pavement testing (APT) provides an economical and beneficial solution to assess the validity of mechanistic-empirical pavement design methods in an environment that closely resembles actual in-service field conditions. Such facilities provide an accurate measure of pavement performance under controlled loading conditions at a relatively moderate cost. Construction practices are the same in real field conditions, and the level of confinement is similar to pavement operating conditions. In addition, incorporation of pavement instrumentation with APT allows the validation of analytical models as well as the calibration of model response variables based on actual field data *[1]*. Pavement instrumentation also helps researchers develop a better understanding of pavement responses, which is essential if accurate design routines are to be suggested. It also contributes to the understanding of the effects of different control variables, such as temperature, moisture, and tire configurations, which are often approximated in current design methods.

Since their introduction in the early 1900s, pavement sensors have evolved considerably and are now capable of providing stable and durable measurements of pavement responses if installed and calibrated properly. Different types of sensors are now available to measure strain, stress, deflection, temperature, frost depth, and moisture. Despite their wide use in accelerated pavement facilities and in full-scale instrumented test sections, only a limited number of studies have been conducted to assess the accuracy, repeatability, and precision of pavement sensors. In addition, long-term accuracy of sensor measurements has not been thoroughly evaluated. This is an important issue in order to quantify pavement performance, given that evolution of damage is the primary indicator of failure progresses in pavement systems. To date, only a few attempts were made to tackle these problems as the scarcity of experimental measurements did not allow for setting a valid ground for assessment.

When instrumenting a pavement structure, response parameters such as vertical stress, horizontal and vertical strains, and deflections are of primary interest. However, environmental parameters such as temperature, frost depth, and moisture content are also needed if pavement response data are to be thoroughly interpreted. For a successful instrumentation strategy, at least two types of response (stress, strain, or deflection) should be compared simultaneously *[2]*. However, earlier research has emphasized the importance of stress and strain measurements to predict pavement performance, given that a direct correlation does not exist between these responses and pavement deflection *[3]*. Unfortunately, accurate measurement of these quantities is a difficult task and requires

adequate selection, calibration, and installation of pavement instrumentation. The following sections provide an overview of pavement stress and strain sensors technology.

**Strain Gages.** To measure strain in flexible pavements, two types of sensors are used depending on the measurement location *[4]*. If measurements are made in bonded layers, electrical resistance strain gages are used; if measurements are conducted in unbonded (granular) layers, linear variable differential transformers (LVDTs) and special strain gages (e.g., vibrating wire strain gage) are typically used. The most important property of a strain gage is its stiffness and variation with temperature *[5]*. An ideal strain gage would have stiffness equal to the stiffness of the surrounding material at all temperatures. In this case, the measured strain will be the true strain in the material. However, since this is never the case, the selected strain gage should have a stiffness that is as close as possible to the ideal case. If the stiffness of the gage is much higher than that of the surrounding material, the sensor will act as reinforcement to the pavement system, and the recorded strain will be much lower than the actual strain in the material.

Strain responses in bituminous layers are usually measured using electrical resistance strain gages. This gage theory of operation is based on the fact that when a thin wire is stretched, its electrical resistance changes. The major problem with this type of gage is its durability. If the high strains that the gage is subjected to during construction exceed its range of operation, it will be damaged or completely destroyed. Therefore, major improvements have been introduced to increase the fatigue and moisture resistance of these gages. The most common types of electrical resistance strain gauge used in bituminous materials are the Kyowa strain gauge, the Dynatest® H-type strain gage, and foil strain gage.

The responses of strain gages installed in bonded materials are very valuable to pavement engineers. Their dynamic responses help engineers gain a better understanding of different control variables, such as vehicle speed, tire pressure, temperature, and so forth. During the last two decades, the qualitative analysis of strain signals in the transverse and longitudinal directions have significantly contributed to the current state of knowledge in pavement engineering *[6]*. Moreover, if quantitative analysis becomes more feasible, the verification of response and performance models would be possible through effective instrumentation.

**Pressure Cell Gages.** Earth pressure cells (also called soil stress gages) consist of a pressure sensor with a transducer to convert the pressure into a measurable signal *[7]*. The most common type of pressure cells is the diaphragm cell. The principle of these transducers is that a pressure acting on the diaphragm of the cell will cause a deflection that can be transformed into an electrical signal by strain gages attached to the inside of the diaphragm

*[3]*. This type of pressure cell has been proven to give a linear response to the applied stress, regardless of the surrounding stiffness.

Two factors affect pressure cell performance: the ratio of the gage thickness to its diameter (aspect ratio) and the ratio of the gage stiffness to that of the surrounding material. Ullidtz found that the recorded and correct stresses will be close if the aspect ratio is very small and the ratio of stiffness very high, which means that the cell should be very stiff compared to the surrounding material *[8]*. Based on Torry et al., the errors in cell measurement will be negligible if the aspect ratio is less than 0.2 *[9]*. Pressure cell installation is the key to good gage performance. However, the accuracy of pressure cells is not well-documented, and a large variability exists among different investigators. The expected accuracy with liquid-filled diaphragm pressure cells is around 25 percent or less *[7]*.

**Evolution of Pavement Damage.** Pavement distresses may be related to a number of factors including traffic, environment, and construction and material deficiencies. Three main HMA distresses are directly related to traffic loading (other factors such as construction deficiencies may contribute to the acceleration of the deterioration): fatigue, rutting, and top-down surface-initiated cracking. While the progress of rutting and top-down cracking damages may be evaluated directly by the increase in damage at the pavement surface, fatigue cracking can only be assessed after failure had occurred and propagated to the surface. Therefore, the use of instrumentation would be mainly beneficial to monitor the progress of fatigue damage prior to its propagation to the surface.

Fatigue cracking is due to the cyclic application of traffic loading. This failure mechanism is usually related to the tensile strain at the bottom of HMA, which can be measured using strain sensors. Under constant wheel loading such as in the case of accelerated loading facility, the progress of pavement damage consists of three main stages *[10]*: (1) initial reorientation of the material, (2) steady state fatigue crack growth in which the evolution of fatigue damage is fairly constant, and (3) unstable crack growth in which the rate of damage increases rapidly as failure is imminent. Under constant stress amplitude such as in APT, tensile strain in the material is expected to gradually increase while stiffness would gradually decrease as cyclic softening of HMA is observed. It is worth noting that fatigue damage may result without any visible sign of cracking as the result of the growth of micro-cracks and the gradual loss of cohesion of the mix under repeated loads *[11]*.

**Laboratory Test Methods**

A number of laboratory tests were conducted in this study to establish the relationship between asphalt deformation properties at low and intermediate temperatures and mix performance. The following sections provide an overview of these test methods.

**Asphalt Ductility Test.** The ductility test, which was introduced in 1903, is conducted by stretching a dog-bone shaped asphalt sample at a constant elongation rate of 5 cm/min. until failure. A number of researchers have established the relationship between asphalt ductility and pavement performance. Halstead found that binders with low ductility are more likely to show poor pavement performance *[12]*. Kandhal and Koehler also found that high asphalt ductility, measured at 15.6$^{o}$C after six years in service, is associated with adequate performance against load-associated longitudinal cracking *[13]*. Despite these past findings, asphalt ductility has been dropped by most state agencies in the U.S., while still being widely used in Europe.

**Direct Tensile Test.** The DTT is used to measure the tensile failure properties of asphalt binder at low temperatures. When introduced in 1992, this test system was expensive, required a nitrogen-based cooling system, and was beset with mechanical problems, which affected the repeatability of the results. After several modifications, a new Superpave DTT was introduced in 1995. The new system, which is very compact compared to the original system, utilizes a fluid-based temperature control system and was reported to produce accurate results *[14]*. This test is currently used as a referee test if the binder stiffness from the bending beam rheometer (BBR) results is between 300 and 600 MPa. If the failure strain is greater than 1 percent, the binder is still accepted even though it may not pass the BBR stiffness criterion since it would be expected to provide sufficient elongation at low temperature. Dongre and co-workers evaluated the relationship between results of DTT and pavement performance at low temperatures *[15]*. Results showed that failure strain data are the best predictors of field performance at low temperatures. While measured BBR stiffness adequately predicted good performers, it failed to identify poor performers in the field.

**High Pressure Gel Permeation Chromatography (HP-GPC).** HP-GPC separates the components of asphaltic materials based on their differences in molecular weights and, therefore, determines the fractions of polymers if present (high molecular weight, HMW), asphaltenes (medium molecular weight, MMW), maltenes (low molecular weight, LMW), and very light oils (very low molecular weight, VLMW) in the binder *[16]*. This process is conducted by introducing a solvent (Tetrahydrofuran) flowing at high pressure through a column of highly porous materials. The liquid transfers the asphalt sample through the

column allowing low molecular weight components to penetrate the pores while heavy components travel more rapidly through the column. A detector determines the fraction of components appearing at a given elution time. As demonstrated in this study, HP-GPC results may be used to relate the fractional compositions of the binder to its physical properties and to determine the impact of the aging process on the rheological behavior of the binder. Past research using HP-GPC of recycled crumb rubber-modified binders has shown that the aging process causes an increase in heavy molecular weight components and a decrease in low molecular weight components *[17]*.

**Differential Scanning Calorimetry (DSC).** The DSC method is widely used for determination of thermal transitions brought about by the first order transitions, such as melting and the crystallization of crystallizable species. The glass transition temperature, $T_g$, credited as a second order phenomenon taking place in the amorphous region of the sample, can be also defined by DSC, but it depends largely on the nature of the material and its content of crystallizable fractions. By allowing the temperature to oscillate in a sinusoidal fashion, a clear distinction can be made on the short time scale of the transition between non-reversible phenomena, such as the first order transitions and reversible glass transition *[18]*.

**Dynamic Mechanical Analysis (DMA).** The DMA technique allows one to characterize the variation of the dynamic complex modulus (E*) and its components (E', E", and tanδ) with temperature. In this test, a beam sample is subject to a cyclic, torsional strain-controlled loading while the temperature is linearly decreased until failure occurs. The glass transition can be detected using DMA by identifying the temperature at which E" peaks at a given frequency. While DSC can be used to measure the glass transition temperature, DMA is more sensitive to thermal changes for amorphous materials such as asphalt binder where the content of crystallizable fraction is not significant. While the use of DMA in asphalt rheology has been limited, Lytton and co-workers evaluated the rate of damage accumulation in asphalt binder and mastic using DMA. Results of this test were found to correlate relatively well with mix performance against moisture damage in the field *[19]*.

**Dynamic Shear Rheometer Test.** The DSR test is typically used to measure the linear viscoelastic moduli of asphalt binders in a sinusoidal loading mode *[20]*. However, the DSR was used in this study to conduct the multiple stress creep recovery (MSCR) test. In this test, a creep shear stress is applied for 1sec followed by a 9-sec rest period. During each cycle, the asphalt binder reaches a peak strain and then recovers before the shear stress is applied again. The DSR operation is simple: the asphalt binder is sandwiched between two parallel plates, one that is fixed and one that oscillates; as the plate oscillates, the sample is

subjected to a defined strain or stress that is resisted by the material through its shear strength.

Dynamic shear rheometer test may be conducted in two ways: controlled-stress and controlled-strain. A controlled-stress test applies a sinusoidally varying stress and measures the magnitude and phase of the resulting strain. A controlled-strain test applies a sinusoidally varying strain to the sample and measures the magnitude and phase of the resulting stress. Two sample sizes are used depending on the testing temperature: a sample with a 25-mm diameter and a thickness of 1 mm is used for high temperatures (46 to 82°C) and a sample with an 8-mm diameter and a thickness of 2 mm is used for intermediate temperatures (4 to 40°C).

**The Indirect Tensile Strength (ITS) Test.** The ITS test (AASHTO T245) is one of the most popular test methods used to characterize asphalt mixtures in the laboratory. It consists of loading a cylindrical specimen with a gradually increasing compressive load until failure. While the specimen is loaded in compression, the loading configuration results in tensile failure in a plane perpendicular to the direction of the load. This test setup allows measuring the tensile strength of the mixture, which is accepted as an indicator against cracking. The tensile strain at failure is also useful in assessing the mixture resistance against cracking. Asphalt mixtures with high strain at failure were found to resist cracking better than mixtures that are more brittle with low tensile strain at failure *[21]*. The tensile stress and strain at failure are calculated as follows:

$$\sigma_f = \frac{2P_f}{\pi dt} \quad (1)$$

$$\varepsilon_f = 0.0205 x_t \quad (2)$$

where,

$\sigma_f$ = horizontal tensile strength at failure (psi),

$P_f$ = load at failure (lb.),

$\varepsilon_f$ = horizontal strain at failure (in/in),

$t$ = thickness of specimen (in.),

$d$ = diameter of specimen (in.), and

$x_t$ = horizontal deformation across specimen (in.).

# OBJECTIVES

The objectives of this study were two fold. First, instrument responses in past ALF experiments were analyzed to quantify variation of pavement responses with temperature and its relationship to pavement performance. Measurements were also used to determine the repeatability of stress and strain measurements in past experiments and the use of sensors technology to assess the evolution of pavement damage. Results of this analysis were used to suggest possible modifications to the instrumentation strategy in future ALF experiments and to develop a successful instrumentation plan for these experiments. This strategy would attempt to ensure repeatable and accurate measurements of pavement responses.

Second, the relationship between the binder deformation properties at intermediate and low temperature and mix performance was established. If asphalt binder performance prediction from the ductility and the direct tensile tests are equivalent, current binder specifications may be modified to require testing using the Superpave DTT instead of relying on the ductility test. This would ensure consistent binder specifications with neighboring states, where straight binder is often obtained.

# SCOPE

The first objective of this study was achieved by reviewing and analyzing collected instrument responses from several prior ALF experiments and quantifying the impacts of temperature variations on instrument responses and on the measured pavement performance. The second objective of this study was achieved by testing nine straight binders obtained from two asphalt suppliers using the ductility test at intermediate temperature, the direct tensile test at low temperature, and the multiple stress creep recovery using the dynamic shear rheometer. To assess the results of these tests, selected asphalt binders were also evaluated using High Pressure Gel Permeation Chromatography (HP-GPC), Dynamic Mechanical Analysis (DMA), and Differential Scanning Calorimetry (DSC). To relate binder properties to mix performance, three of the nine binders with contrasting levels of ductility were used to prepare hot-mix asphalt specimens, which were tested using the indirect tensile strength test.

# METHODOLOGY

## Accelerated Loading Facility Experiments

### The Louisiana Accelerated Loading Facility

The Louisiana ALF is a full-scale transportable pavement test device that simulates the effect of traffic loading on full-scale pavement by applying controlled wheel loading in a repetitive manner *[22]*. This setup has the same design as the ones located at the Turner-Fairbanks Highway Research Center; however, temperature at the ALF is not controlled during testing. This loading system applies a constant truck wheel load at a speed ranging from 8 to 12 mph. The loading length of the ALF is 85 ft. with approximately 33 ft. of constant velocity loading of the wheel. The load applied on the pavement can be varied from a dead weight of 10 kip to 25 kip by adding static load plates.

**Figure 1**
**The Louisiana accelerated loading facility**

### Test Sections

This research project dealt with the results of Experiments II and III. Experiment II was designed and constructed to evaluate the performance of asphalt rubber (AR) as compared to conventional HMA and to determine the optimum location of the asphalt rubber layer within

the pavement structure *[22]*. Three test lanes, each 215 ft. x 13 ft., were constructed for this experiment. In the first lane, asphalt rubber was used in the surface layer, while asphalt rubber was used in the base mixture layer in the second lane, and lane 3 was the control section consisting of conventional asphalt mixes throughout the layers. Figure 2 illustrates the pavement design and instrumentation strategies in these test lanes.

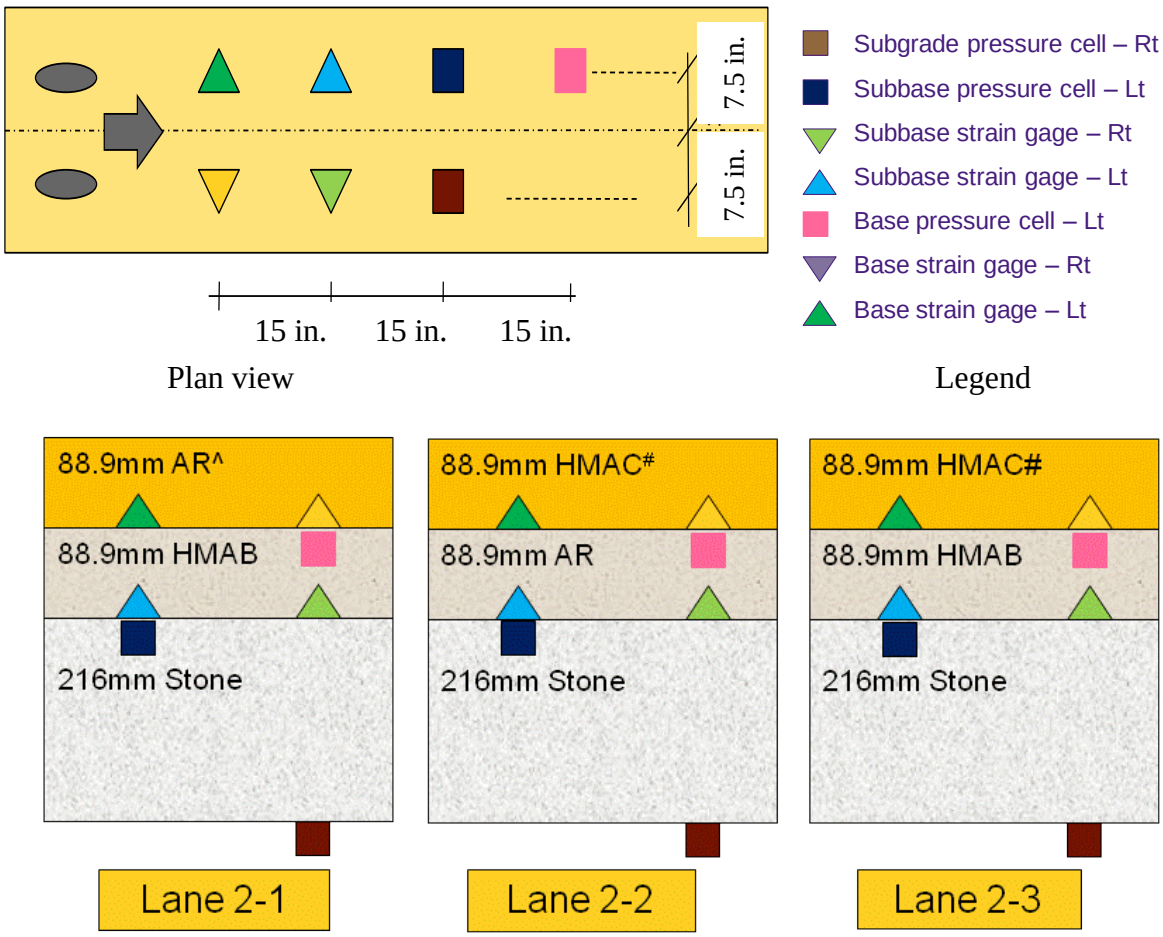


^ = surface layer consists of 1.5 in. AR-HMA wearing course on top of 2 in. conventional binder course. # = surface layer consists of 1.5 in. conventional wearing course on top of 2 in. conventional binder course.

**Figure 2**
**Pavement design and instrumentation plan in Experiment II**

Experiment III was designed and constructed to evaluate the feasibility of using reclaimed asphalt pavement (RAP) materials as an aggregate interlayer *[23]*. Three test lanes, each 215 ft. x 13 ft., were constructed for this experiment. In the first lane, a RAP interlayer was used in the base layer on top of a 10-in. subgrade layer stabilized with 5 percent cement; in the second lane, a RAP interlayer was installed on top of a 6-in. subgrade layer stabilized with 10 percent cement; in the third lane (control section), a conventional stone base layer was placed

on top of a 10-in. subgrade layer stabilized with 10 percent cement. Results of the evaluation of the effectiveness of the RAP interlayer as a stress-relieving layer between a cement-treated base and HMA, in lieu of crushed stone, have been presented elsewhere *[24]*. Figure 3 illustrates the pavement design and instrumentation strategies in these test lanes.

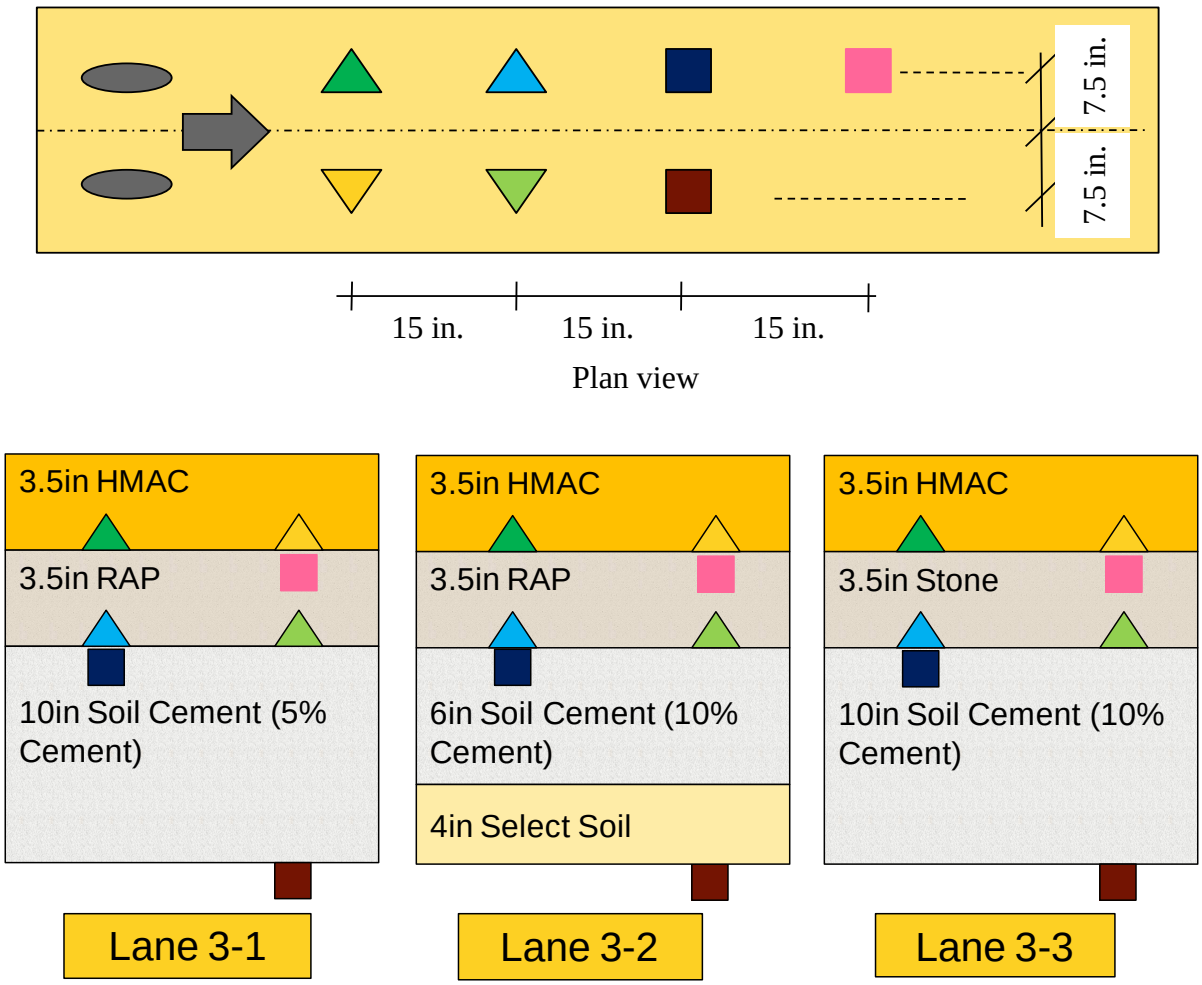


**Figure 3**
**Pavement design and instrumentation plan in Experiment III**

**Instruments Description**

Load-associated instruments included pressure cells and strain gages, which were installed at the bottom of the different pavement layers. Pressure cells, manufactured by Geokon, were used to measure vertical stress in the pavement system in Experiments II and III (Figure 4). This sensor consists of two circular steel plates welded together around their rims to create a cell approximately 9 in. in diameter and 0.25-in. thick, which results in an aspect ratio well below the threshold recommended by Torry et al. *[9]*. External pressure acting on the cell is balanced by an equal pressure induced in an internal fluid placed inside the gage. This

sensor has a pressure range of up to 100 psi. The responses of Tokyo Sokki Kenkyujo Co. (TML) model KM-100-HAS strain gages were used in Experiments II and III to measure the longitudinal strain in the pavement structure (Figure 4). This model is a full bridge, with a 350 Ω resistance and a strain capacity of ± 5,000 μstrain. These gages were reported to provide excellent durability and robustness with a survivability rate of 96 percent during the paving process *[25]*.

**Figure 4**
**Pressure cells and strain gages used to measure pavement responses**

**Instrument Installation**

All instruments were embedded in the pavement sections during construction. Instruments were placed 15 in. apart in the longitudinal direction and 7.5 in. from the centerline of the lane in the transverse direction. Pressure cells were installed so that the bottom side was leveled with the top of the layer where stress measurements were to be made during the experiment (Figure 5). A hole was dug to accommodate the fluid-housing unit of the pressure cell, and the gage was then leveled in its position. Any angular aggregates were manually removed to protect the sensitive side of the gage. A thin layer of sand was then placed beneath the sensitive side to avoid tilting of the gage during construction.

**Figure 5**
**Installation of pressure cells at the ALF facility**

Installation of the H-type strain gages was a delicate operation, Figure 6. When gages are installed in a HMA layer, as in these experiments, they can be subjected to very large strains during compaction of the pavement layer. After installation, the major problem involves damage caused by moisture. The gages may also suffer from fatigue before the HMA does. During installation, correct alignment and leveling of the gage was first checked. A small quantity of binder was then poured around the gage to ensure correct alignment and that the gage would not move during construction. Loose mixture was then placed on top of the gage and manually compacted to provide a protective layer against direct contact with the paver and excessive compaction effort. Vibration was not allowed within approximately 5 ft. from the gage location.

**Figure 6**
**Installation of the strain gages at the ALF facility (Experiment III)**

**Testing Process**

A dual 11R22.5 radial ply truck tire that was maintained at a pressure of 105 psi was used to load the test lanes at a constant speed of 10 mph with a wander distribution of ± 15 in. around the lane centerline, Figure 1. On average, 35,000 repetitions were applied per week. The loading schemes adopted in Experiments II and III are presented in Table 1. It was estimated that approximately $5.5 \times 10^6$ Equivalent Single Axle Loads (ESALs) were applied over the course of Experiment II and $2.3 \times 10^6$ ESALs in Experiment III. As shown in Table 1, the loading process took place from March 1999 to December 2000 (one year and nine months) in Experiment II and from April 2001 to January 2004 (two years and eight months) in Experiment III. Loading was applied alternatively between the test lanes in 25,000 pass increments in an attempt to minimize environmental effects and seasonal variation between the test lanes. Rutting measurements were conducted after each increment of 25,000 load applications using the ALF profilograph. A rutting ranging between 0.5 and 0.75 in. was defined as the failure criterion for the pavement structure.

**Table 1**
**Loading process in Experiments II and III *[24], [26]***

| Experiment | Load (lbs) | Number of Passes (x1000) | Cumulative ESALs | Date Load First Applied |
|---|---|---|---|---|
| Exp. II | 9,750 | 0 – 400 | 550,800 | 03/99 |
| | 12,050 | 400 – 500 | 872,100 | 10/99 |
| | 14,340 | 500 – 650 | 1,841,550 | 12/99 |
| | 16,630 | 650 – 750 | 3,012,850 | 04/00 |
| | 19,000 | 750 – 800 | 3,995,600 | 10/00 |
| | 21,220 | 800 – 850 | 5,549,550 | 12/00 |
| Exp. III | 9,750 | 0 – 200 | 275,473 | 04/01 |
| | 12,050 | 200 – 525 | 1,319,794 | 05/02 |
| | 14,340 | 525 – 675 | 2,289,252 | 01/04 |

## Laboratory Testing

A number of laboratory tests were conducted to establish the relationship between asphalt deformation properties at low and intermediate temperatures and mix performance. The following sections describe the test procedures and the sampled asphalt materials.

### Test Materials

**Asphalt Binder.** The experimental program was designed to evaluate a wide range of asphalt binders with contrasting levels of ductility. Nine unmodified binders from two major asphalt suppliers (seven from one supplier and two from a second supplier) that are classified as PG 64-22 according to the Superpave specifications were selected (Table 2). These binders were labeled A, B, and so on until I. As shown in Table 2, it is noted that all binders satisfied the Superpave binder specification requirements for PG 64-22. Samples were obtained from the asphalt suppliers in the virgin state and were then processed for short-term and long-term aging (i.e., rolling-thin film oven [RTFO], and pressure-aging vessel [PAV]).

**Table 2**
**Asphalt binder characteristics**

| Binder ID | G*/sinδ (64°C) Original – kPa | G*/sinδ (64°C) RTFO – kPa | G*sinδ (25°C) PAV – kPa | BBR Stiffness (MPa) | m-value | Brookfield @135°C |
|---|---|---|---|---|---|---|
| A | 1.74 | 4.66 | 2430 | 113 | 0.350 | 0.550 |
| B | 1.73 | 5.22 | 2120 | 87 | 0.355 | 0.560 |
| C | 1.67 | 4.31 | 2460 | 107 | 0.334 | 0.530 |
| D | 1.77 | 5.79 | 1793 | 127 | 0.332 | 0.530 |
| E | 1.55 | 4.60 | 2520 | 94 | 0.351 | 0.520 |
| F | 1.57 | 4.29 | 3000 | 108 | 0.333 | 0.530 |
| G | 2.09 | 4.81 | 4855 | 229 | 0.311 | 0.545 |
| H | 2.03 | 4.67 | 4550 | 218 | 0.313 | 0.563 |
| I | 1.89 | 3.90 | 4804 | 231 | 0.312 | 0.588 |

**Asphalt Mixture.** To determine the impacts of the binders' elongation properties on the mix performance at intermediate temperature, a limited number of mix samples were prepared and tested using the Indirect Tensile Strength test. Using this test setup, the mixture tensile strength and the horizontal strain at failure were measured. The adopted mix design followed the guidelines developed by Mohammad et al. to prepare a low-cost asphalt-treated base mixture *[27]*. This mixture consists of 25 percent coarse sand, 75 percent coarse

aggregate (Martin Marietta Limestone), 3 percent binder, and is compacted at 30 gyrations. Three binder types were used in the preparation of 18 cores (3 binders x 2 aging conditions x 3 replicates). The selected binders were binders B, F, and G (Table 2). Binder G had the highest ductility, Binder B had the lowest ductility, and Binder F had an intermediate level of ductility. Mixtures were tested in the unaged and aged conditions. Long-term aging of the mixture was simulated by placing the compacted cores in the oven at 85 ± 3°C for 120 hours.

**Ductility Test**

The ductility test was conducted according to AASHTO Specification T 51-06 by stretching a dog-bone shaped asphalt sample at a constant elongation rate of 5 cm/min. until failure (Figure 7). This test was conducted in a water bath maintained at a standard temperature of 25$^{o}$C. Results of this test were used to assess the ability of straight asphalt binder to stretch without breaking. This is an important property sought in asphalt binder at low and intermediate temperatures to avoid premature initiation of micro-cracks in the asphalt film due to repetitive thermal and vehicular loading. Louisiana asphalt binder specifications require that Rolling-Thin Film Oven (RTFO) PG 64-22 binder residue used in the state provides a minimum elongation of 100 cm as measured by the ductility test. Three replicates were concurrently tested, and the average elongation at failure was reported.

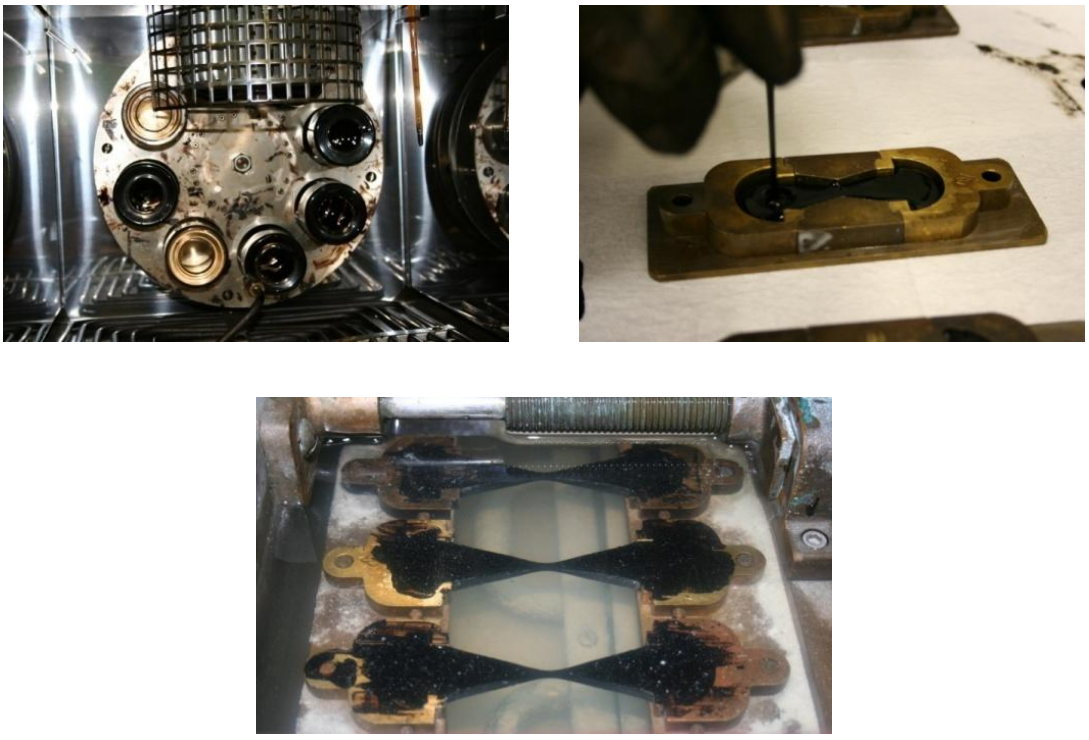

**Figure 7**
**Illustration of the ductility test**

**Direct Tensile Test**

The DTT was used to measure the tensile failure properties of asphalt binder at a low temperature (-12$^{o}$C). This test was conducted by pulling a dog-bone shaped asphalt sample at an elongation rate of 1 mm/min. until breakage, Figure 8. The load developed during the test is measured, and the tensile strain and stress in the specimen at failure are reported. This test is currently not used in Louisiana for specification purposes. However, other states used it as a referee test if the binder stiffness from BBR results is between 300 and 600 MPa. If the failure strain is greater than 1 percent, the binder is still accepted even though it may not pass the BBR stiffness criterion since it would be expected to provide sufficient elongation at low temperatures. AASHTO specification (T 314-02) requires to test six replicates of Pressure Aging Vessel (PAV) aged asphalt binder residue and to calculate the failure strain based on the results of the four specimens with the highest failure strain *[28]*.

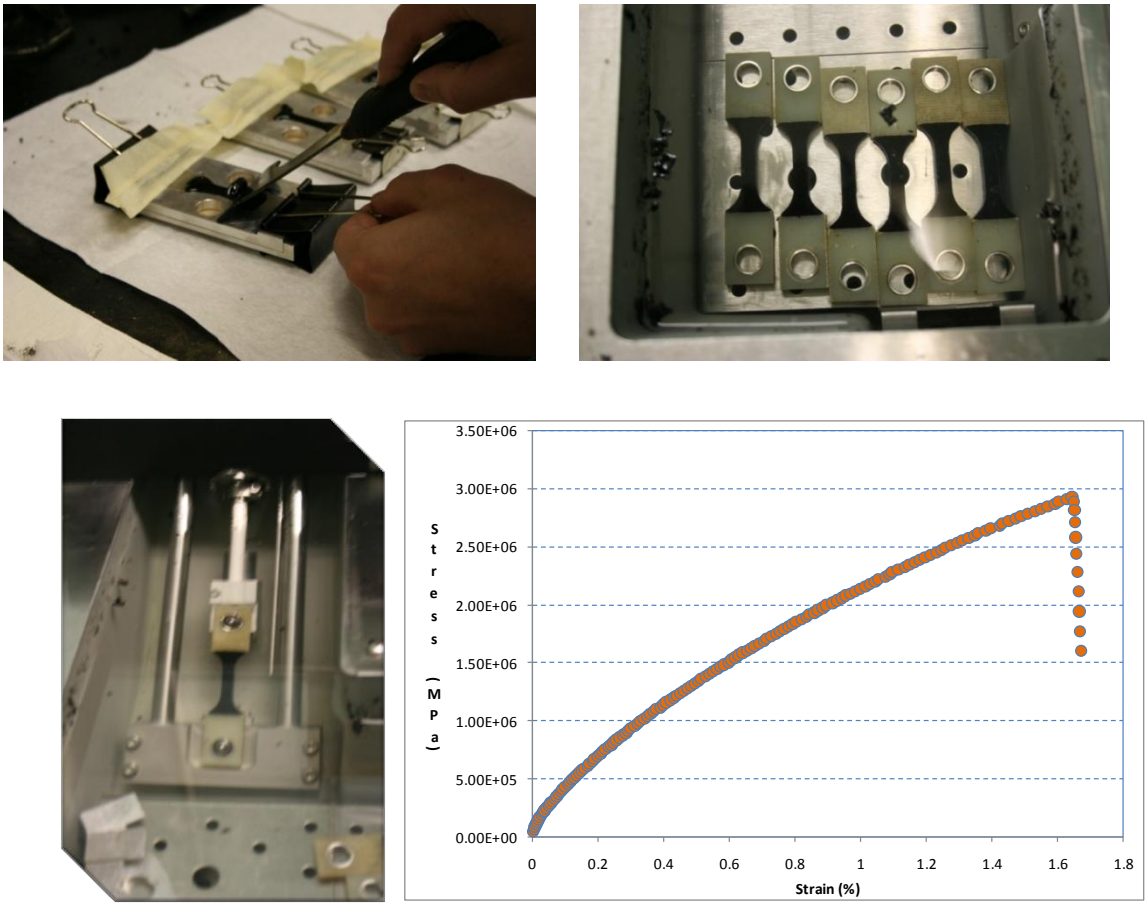


**Figure 8**
**Illustration of the direct tensile test and typical results from the test**

**High Pressure Gel Permeation Chromatography**

HP-GPC was conducted for the selected binders in all aging conditions. A gel permeation chromatograph Agilent 1100 equipped with an auto injector and a Hitachi differential refractive index detector was used. The separation of the asphalt components was performed with three columns connected in series with pore sizes of 500 Å (1-15 K), 10-4 Å (5-500 K) and mix bids (100-10,000 K). The column set was calibrated with narrow molecular weight polystyrene (PS) standards using 3 percent weight concentration of tetrahydrofuran (THF). The molecular weight elution volume for polystyrene standards was used to build a linear calibration curve. All asphalt samples for GPC were prepared at a concentration of 3 percent in THF, injected through a 0.45µ filter into 150 µL vials, and inserted in an automatic injector. Samples were eluted with THF at 1 ml/min. at room temperature, and the species concentration in the eluent was recorded using a differential refractometer. The GPC curves were integrated, and the areas were normalized over the total area of the chromatogram. The expected error in the measured molecular fractions is around 0.2 percent or less.

**Differential Scanning Calorimetry**

The presence of crystallizable species was determined using DSC for the selected asphalt binders (considered mostly as paraffinic maltenes). These measurements were conducted using a TA 2920 MDSC V2.6A module with the following testing parameters: 5-10 mg sample and a heating rate of 2°C/min. with a modulation program of 0.5°C at each 0.4 min.

**Dynamic Mechanical Analysis**

An ARES rheometer was used for dynamic mechanical analyses of the selected asphalt binders in order to determine the glass transition temperature. The following test parameters were used: torsion (twisting) in a cooling mode; sample dimensions: 3 mm x 13 mm x 15 mm; cooling rate: 1°C/min.; frequency: 1 Hz; sinusoidal cyclic strain with an amplitude of 1 percent.

**Multiple Stress Creep Recovery Test**

The multiple stress creep recovery (MSCR) test was conducted in this study to determine whether it may be used as a predictor of binder ductility. As it was previously noted, DSR is already used in the current Superpave binder specification in Louisiana, and the validity of this relationship would allow substituting the ductility conventional test with a Superpave-related test. In this test, the dynamic shear rheometer is used to apply a constant shear stress for 1 sec. followed by a 9-sec. rest period. This test was recently introduced to characterize the binder rutting resistance at high temperatures. It was reported to correlate well with the mixture rutting performance as measured by accelerated pavement testing *[29]*. It can also be used to determine the stress dependency of polymer modified binders. Two performance

parameters have been suggested to evaluate the binder performance at high temperature. The non-recoverable creep compliance ($J_{nr}$) normalizes the strain response of the binder to stress as follows:

$$J_{nr} = \frac{\varepsilon_{nr}}{\sigma} \quad (3)$$

where,

$J_{nr}$ = non-recoverable creep compliance (1/kPa),

$\varepsilon_{nr}$ = non-recoverable strain at the end of the rest period, and

$\sigma$ = constant stress applied in the creep phase of the test (kPa).

The percentage recovery at the end of the recovery period is also determined as follows:

$$\varepsilon_r = \frac{\varepsilon_1 - \varepsilon_{10}}{\varepsilon_1} x100 \quad (4)$$

where,

$\varepsilon_r$ = percentage recovery,

$\varepsilon_1$ = strain at the end of the creep phase (after 1 sec.), and

$\varepsilon_{10}$ = strain at the end of the recovery period (after 10 sec.).

The test is conducted for 10 consecutive load cycles, and the average non-recoverable creep compliance and percentage recovery is calculated over these 10 cycles. For acceptable performance, it is desirable to use a binder with a low, non-recoverable creep compliance and high percentage recovery. At high temperature, two standard stress levels are typically used (100 Pa and 3200 Pa) to determine the stress dependency of the binder. The stress dependency is predicted by calculating the percentage difference in the binder response at the two stress levels as follows:

$$\varepsilon_{r-difference} = \frac{\varepsilon_{r100} - \varepsilon_{r3200}}{\varepsilon_{r100}} x100 \quad (5)$$

where,

$\varepsilon_{r-difference}$ = percentage difference in recovery between 100 Pa and 3200 Pa,

$\varepsilon_{r100}$ = percentage recovery at 100 Pa, and

$\varepsilon_{r3200}$ = percentage recovery at 3200 Pa.

Since the MSCR test was performed in this study to establish its relationship to the ductility test, it was conducted at 25$^{o}$C on RTFO-residues. Therefore, linearity tests were conducted to determine suitable stress levels at this temperature. Linearity and MSCR tests were conducted using an AR2000 rheometer that was set up to work in the Dynamic Shear Mode. Figure 9 presents the main components of this rheometer. Linearity sweep tests were conducted by gradually increasing the stress level and measuring the strain response of the

binder to each stress level. The linear region was defined at the stress level at which a 5 percent reduction in the complex shear modulus (G*) occurred. Figure 10 (a and b) present typical test results obtained from the linearity test and the MSCR test, respectively.

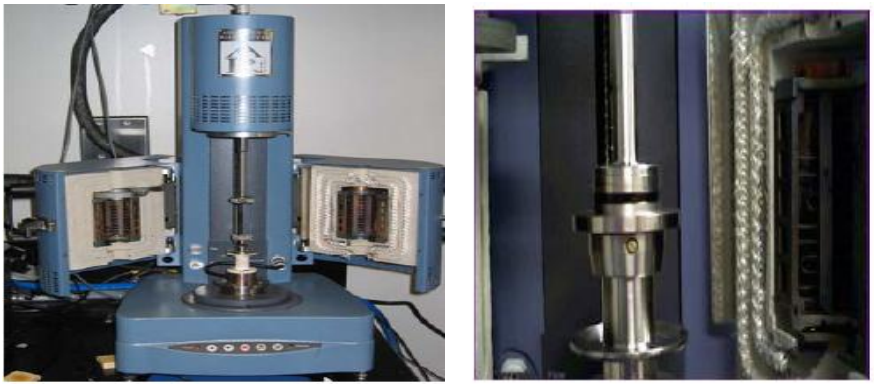

**Figure 9**
**AR 2000 instrument in dynamic shear mode**

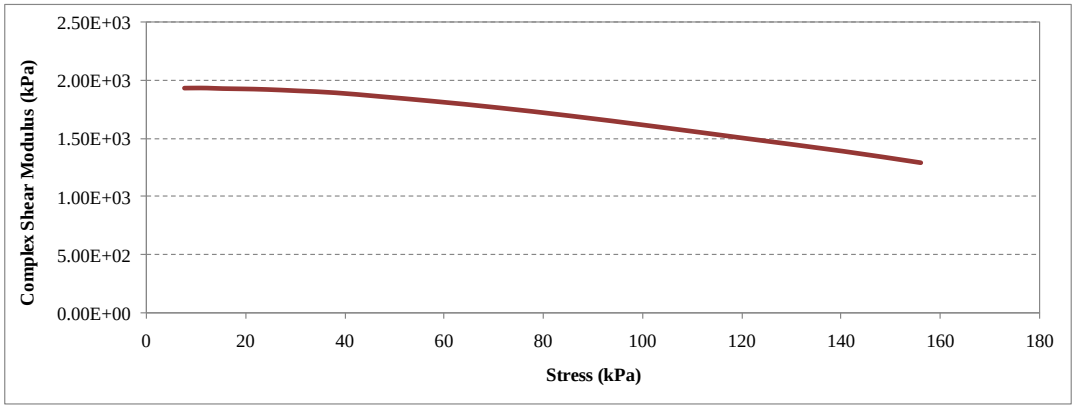


**(a)**

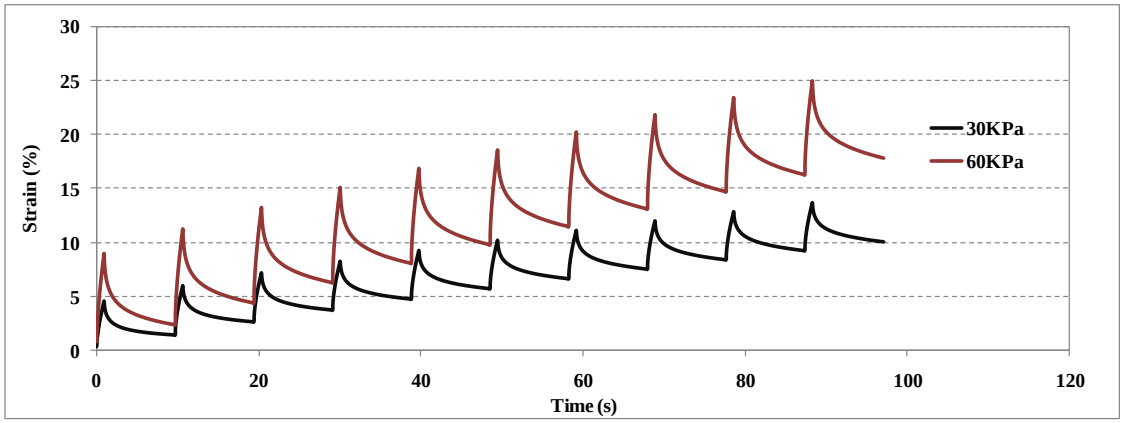


**(b)**

**Figure 10**
**Typical test results obtained from (a) the linearity test and (b) the multiple stress creep recovery test**

# DISCUSSION OF RESULTS

## Analysis of Instrument Responses from Experiments II and III

Field measurements were used to assess survivability and repeatability of stress and strain measurements, seasonal variations, and the use of sensor technology to monitor pavement damage.

### Instrument Responses to Vehicular Loading

Figure 11 (a and b) present typical strain signals measured after 150,224 and 50,921 passes in Experiments II (Lane 2-1) and III (Lane 3-1), respectively. These measurements were made at the bottom of the surface layers in the longitudinal direction at a depth of 3.5 in. as multiple passes were applied directly on top of the sensors. Signals shown in Figure 11 agree with the characteristics of these measurements as reported by past investigators *[30], [31]*. The longitudinal strain response first shows compression, then tension, and finally compression again. The second compression peak is always lower than that of the first, and it was sometimes non-existent in the measurements. The longitudinal strain measurements at the bottom of the surface layers were consistent until approximately 435,000 passes in Experiment II and 350,000 passes in Experiment III; after that, the signals appeared noisier but the peak response could still easily be extracted; see Figure 12.

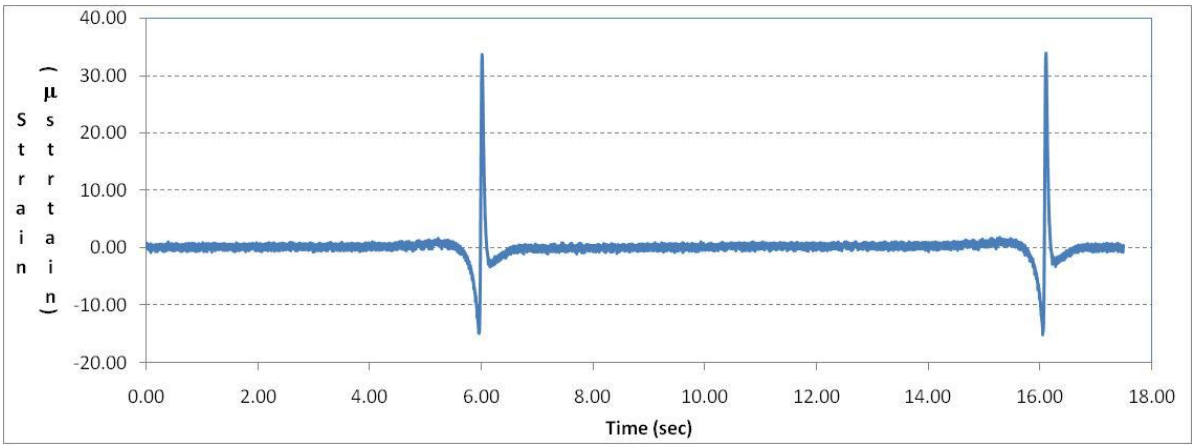


**(a)**

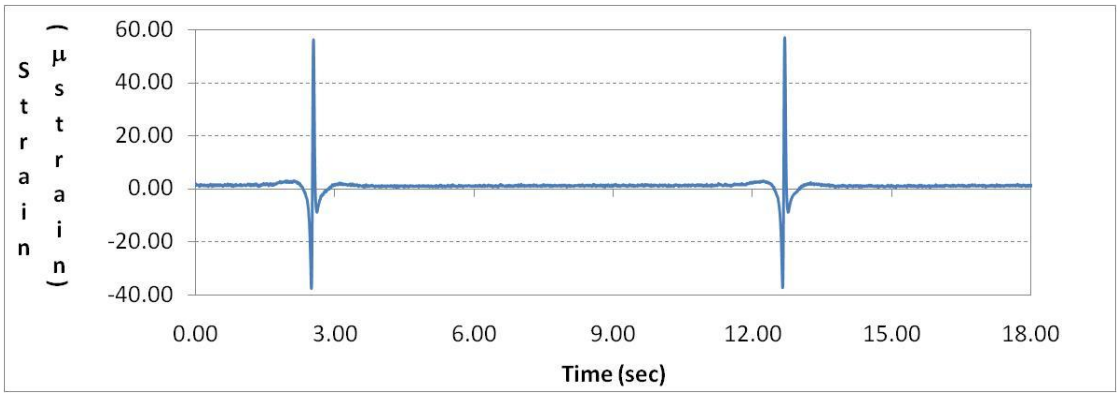


**(b)**

**Figure 11**
**Typical measured longitudinal strain at the bottom of the surface layers (88.9mm) after (a) 150,224 passes (Experiment II) and (b) 50,921 passes (Experiment III)**

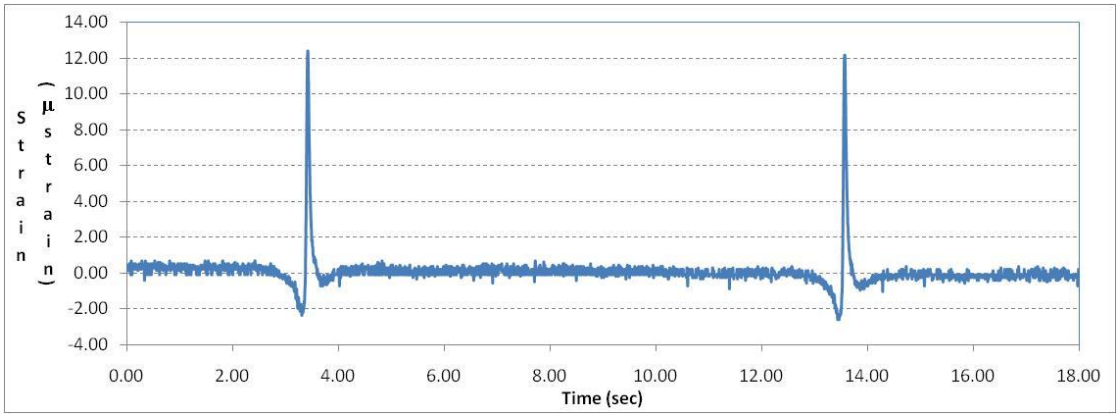


**(a)**

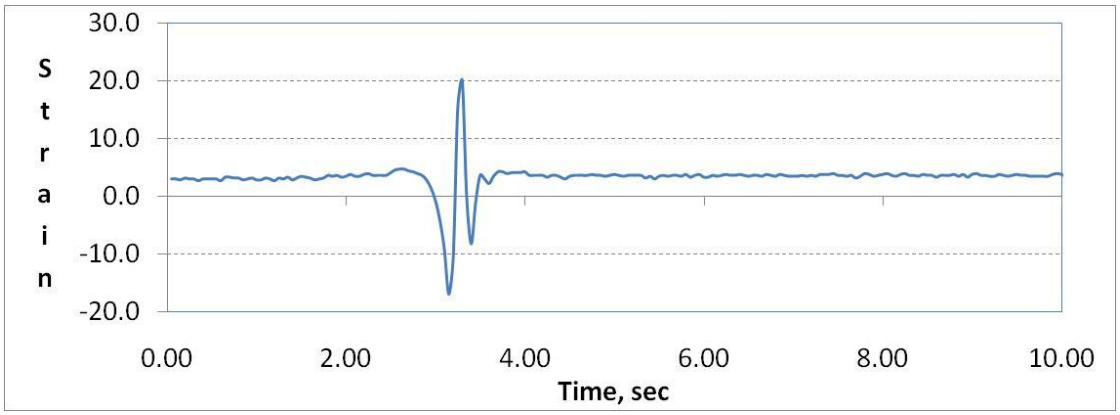


**(b)**

**Figure 12**
**Measured longitudinal strain at the bottom of the surface layers (88.9mm) after (a) 435,000 passes (Experiment II) and (b) 350,000 passes (Experiment III)**

Figure 13(a) presents a typical stress signal measured in Experiment III (Lane 3-1) at a depth of 17.0 in. as multiple passes were applied directly on top of the pressure cell. As expected, mostly compressive stress was measured in the vertical direction. However, one may notice slight vertical shifting in the pressure cell signal as the signal did not originate from zero. A small tension at the beginning and the end of the vertical stress pulse was also observed in some of the responses as the number of passes increased; see Figure 13(b). This may be due to slight tilting or failure of the cell as the number of passes increased or as the load level was raised. Pressure cell data after 225,000 passes in Experiment III were not used in the conducted analysis as they appeared to be doubtful.

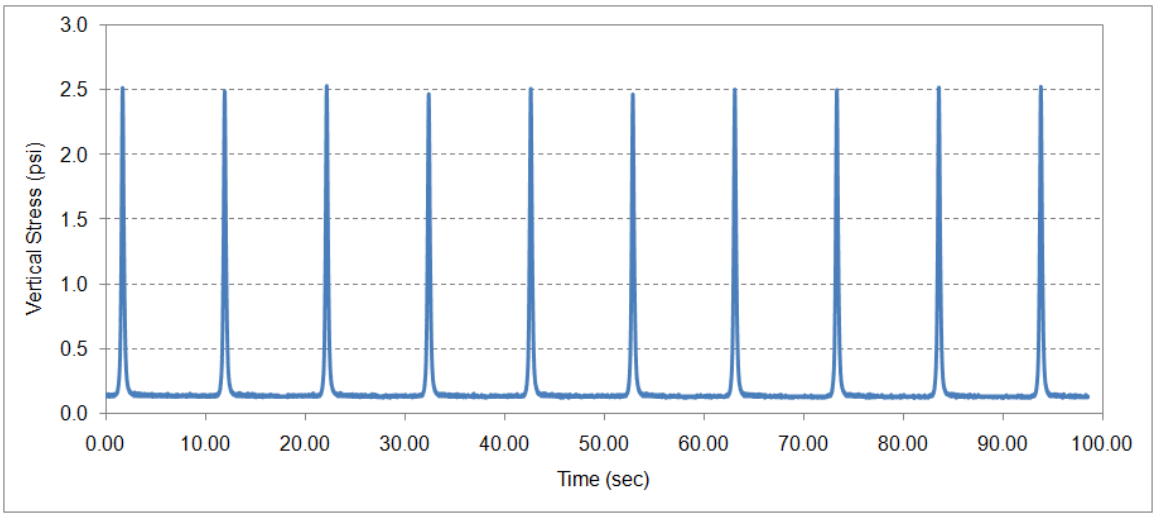


**(a)**

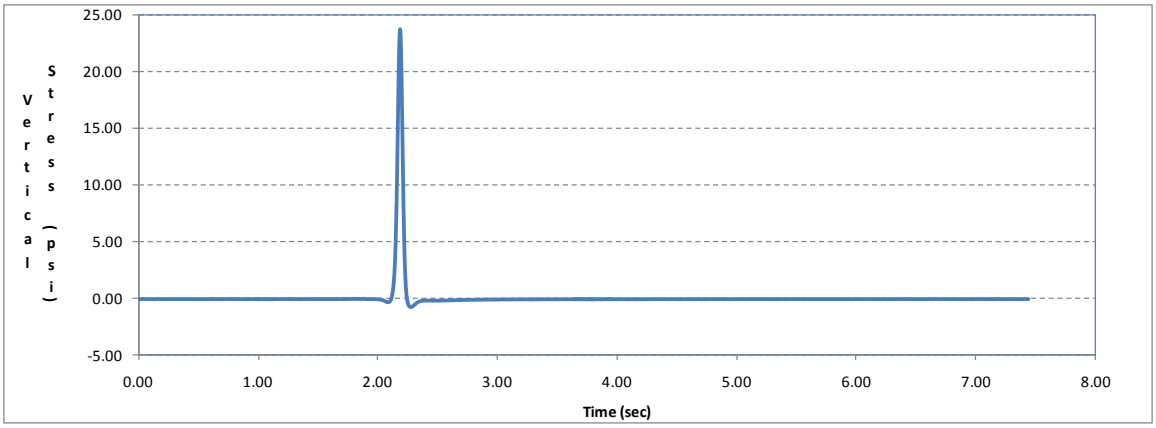


**(b)**

**Figure 13**
**Measured vertical stress in Experiment III (a) on top of the subgrade layer (225,000 passes); (b) at the bottom of the surface layers (200,000 passes)**

In Experiment II, pressure cell responses at the bottom of the surface layers were acceptable until the end of the test program. However, a small jump was observed in the measured signals after 435,000 passes possibly due to tilting of the sensor as the number of passes was increased; see Figure 14.

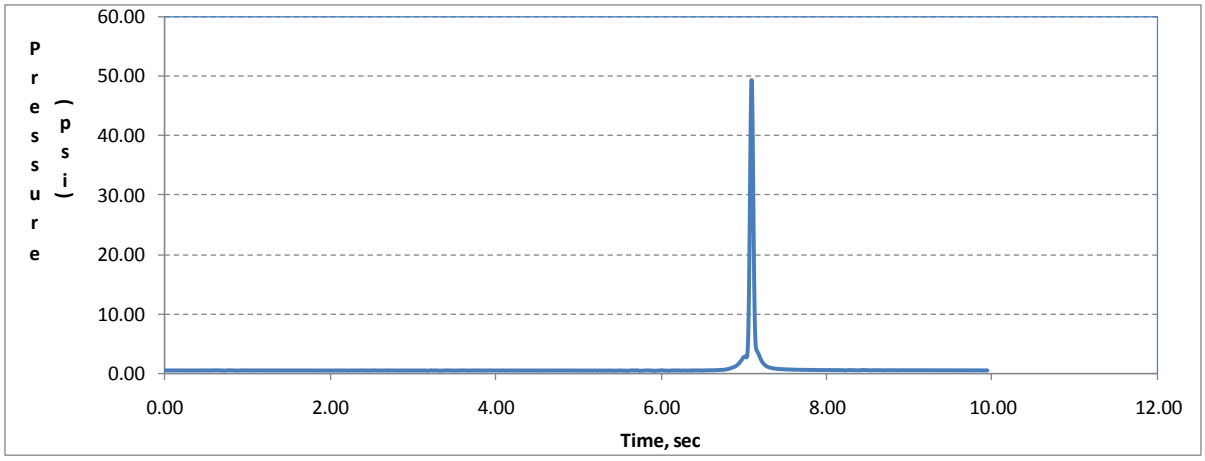


**Figure 14**
**Measured vertical stress in Experiment II at the bottom of the surface layers (565,000 passes)**

**Sensors Survivability**

Table 3 illustrates the survivability ratings of the different sensors in Experiment II and III. It is noted that although some of the gages did not explicitly fail in the experiment, their readings seemed particularly unreliable and did not agree with the characteristics of these signals as reported in the literature. For instance, the base strain gage (Lt) in Lane 2-2 consistently showed a higher level of compressive strain than tensile strain, which was not expected as the reverse trend has been reported *[5], [30]*. Tilting of the pressure sensors indicates that tensile reading or jumps similar to the ones shown in Figure 13(b) and Figure 14 were observed in the measured signals. In general, instrument responses in Lane 1 of Experiments II and III were better quality than the other two lanes in each of the two experiments. Therefore, more emphasis is given to these two lanes in the presented analysis.

**Table 3**
**General survivability performance of pavement sensors in Experiments II and III**

**(a) Experiment II**

| *Lane* | *Sensor* | *Depth (in.)* | *Service Life* | *Notes* |
|---|---|---|---|---|
| 2-1 | Base Strain Gage Lt | 3.5 | Did not fail | Readings failed a couple of times |
| | Base Strain Gage Rt | 3.5 | Did not fail | Readings failed a couple of times |
| | Base Pressure Cell Lt | 3.5 | Did not fail | Jump in the signals after 435 k |
| | Subbase Strain Gage Lt | 7.0 | Did not fail | Good responses |
| | Subbase Strain Gage Rt | 7.0 | Did not fail | Gage stopped working between 150 and 200 k and 200 and 350 k |
| | Subbase Pressure Cell | 7.0 | Did not fail | Started tilting after 501 k |
| | Embankment Pressure Cell | 15.5 | Did not fail | Started tilting from the beginning of the experiment |

| *Lane* | *Sensor* | *Depth (in.)* | *Service Life* | *Notes* |
|---|---|---|---|---|
| 2-2 | Base Strain Gage Lt | 3.5 | Did not fail | Readings were noisy and unreliable from the beginning of the experiment |
| | Base Strain Gage Rt | 3.5 | Failed after 150 k | |
| | Base Pressure Cell Lt | 3.5 | Did not fail | Good responses |
| | Subbase Strain Gage Lt | 7.0 | Did not fail | |
| | Subbase Strain Gage Rt | 7.0 | Did not fail | |
| | Subbase Pressure Cell | 7.0 | Did not fail | Started tilting from the beginning of the experiment |
| | Embankment Pressure Cell | 15.5 | Did not fail | Started tilting from the beginning of the experiment |

| *Lane* | *Sensor* | *Depth (in.)* | *Service Life* | *Notes* |
|---|---|---|---|---|
| 2-3 | Base Strain Gage Lt | 3.5 | Did not fail | |
| | Base Strain Gage Rt | 3.5 | Did not fail | |
| | Base Pressure Cell Lt | 3.5 | Failed after 350 k | Sporadic responses |
| | Subbase Strain Gage Lt | 7.0 | Did not fail | |
| | Subbase Strain Gage Rt | 7.0 | Did not fail | Signals became noisy after 375 k |
| | Subbase Pressure Cell | 7.0 | Did not fail | Signals became noisy after 375 k |
| | Embankment Pressure Cell | 15.5 | Failed from the start | Sensor was lost from the beginning of the experiment |

**(b) Experiment III (Depth in inches)**

| *Lane* | *Sensor* | *Depth* | *Service Life* | *Notes* |
|---|---|---|---|---|
| 3-1 | Base Strain Gage Lt | 3.5 | Did not fail | |
| | Base Strain Gage Rt | 3.5 | Did not fail | |
| | Base Pressure Cell Lt | 3.5 | Did not fail | Readings seem unreliable after 225 k |
| | Subbase Strain Gage Lt | 7.0 | Failed from the start | |
| | Subbase Strain Gage Rt | 7.0 | Did not fail | Readings were unreliable from the beginning of the experiment |
| | Subbase Pressure Cell | 7.0 | Failed after 50 k | Sensor seemed tilted from the beginning of the experiment |
| | Embankment Pressure Cell | 17.0 | Failed after 225 k | Readings were shifted from the beginning of the experiment |

| *Lane* | *Sensor* | *Depth* | *Service Life* | *Notes* |
|---|---|---|---|---|
| 3-2 | Base Strain Gage Lt | 3.5 | Failed from the start | |
| | Base Strain Gage Rt | 3.5 | Failed from the start | |
| | Base Pressure Cell Lt | 3.5 | Did not fail | |
| | Subbase Strain Gage Lt | 7.0 | Failed after 40 k | |
| | Subbase Strain Gage Rt | 7.0 | Failed from the start | |
| | Subbase Pressure Cell | 7.0 | Did not fail | |
| | Embankment Pressure Cell | 17.0 | Did not fail | |

| *Lane* | *Sensor* | *Depth* | *Service Life* | *Notes* |
|---|---|---|---|---|
| 3-3 | Base Strain Gage Lt | 3.5 | Did not fail | Readings were only available for a few numbers of passes |
| | Base Strain Gage Rt | 3.5 | Did not fail | Readings are only available for a few numbers of passes |
| | Base Pressure Cell Lt | 3.5 | Did not fail | Started tilting from the beginning of the experiment |
| | Subbase Strain Gage Lt | 7.0 | Did not fail | Readings were unreliable and were only available for a few passes |
| | Subbase Strain Gage Rt | 7.0 | Did not fail | Readings were only available for a few numbers of passes |
| | Subbase Pressure Cell | 7.0 | Did not fail | Started tilting from the beginning of the experiment |
| | Embankment Pressure Cell | 17.0 | Failed from the start | |

**Strain Measurements Repeatability**

Figure 15 (a and b) presents the measured longitudinal strain throughout Experiments II (Lane 2-1) and III (Lane 3-1), respectively. The two strain gages presented in each of these figures are at the same depth of 3.5 in. (at the bottom of HMA layers). However, one of the strain gages (Base Strain Lt) was placed underneath the left wheel of the dual tire while the second strain gage (Base Strain Rt) was placed underneath the right wheel. As shown in these figures, these sensors provided the same trend of measurements in which considerable

variation is noticed due to seasonal variations (i.e., increase in strain during the summer seasons) and increase in number of passes (i.e., overall decrease in the strain measurements).

The average coefficient of variation between the two sets of measurements shown in Figure 15(b) was 7.5 percent. However, variation in Experiment II was much higher with an average coefficient of variation of 26.4 percent. Review of the individual responses in Experiment II did not indicate a clear explanation for this difference; however, strain measurements in Experiment II were somewhat lower in magnitude than in Experiment III, which may have resulted in greater variability in the responses. A statistical analysis of variance was conducted between the two sets of measurements from Experiment III and revealed that the two data groups are not statistically different (Number of observations = 21, F = 0.62, $F_{critical}$ = 4.1, and P = 0.43).

As expected, this analysis also revealed that the two sets of measurements from Experiment II presented in Figure 15(a) are statistically different (Number of observations = 26, F = 8.51, $F_{critical}$ = 4.03, and P = 0.005).

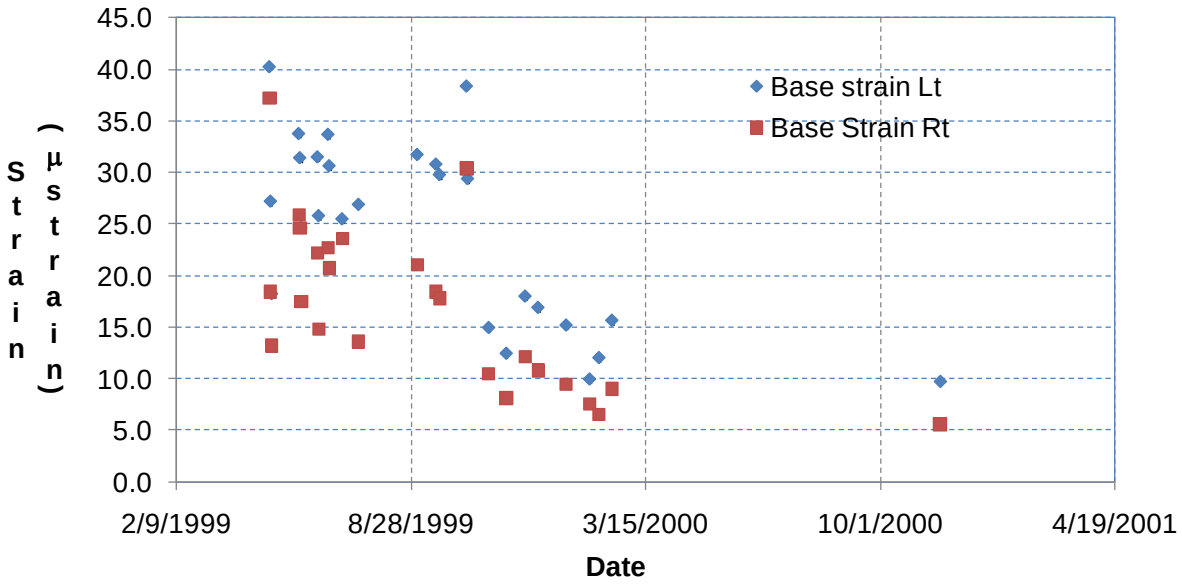


**(a) Experiment II**

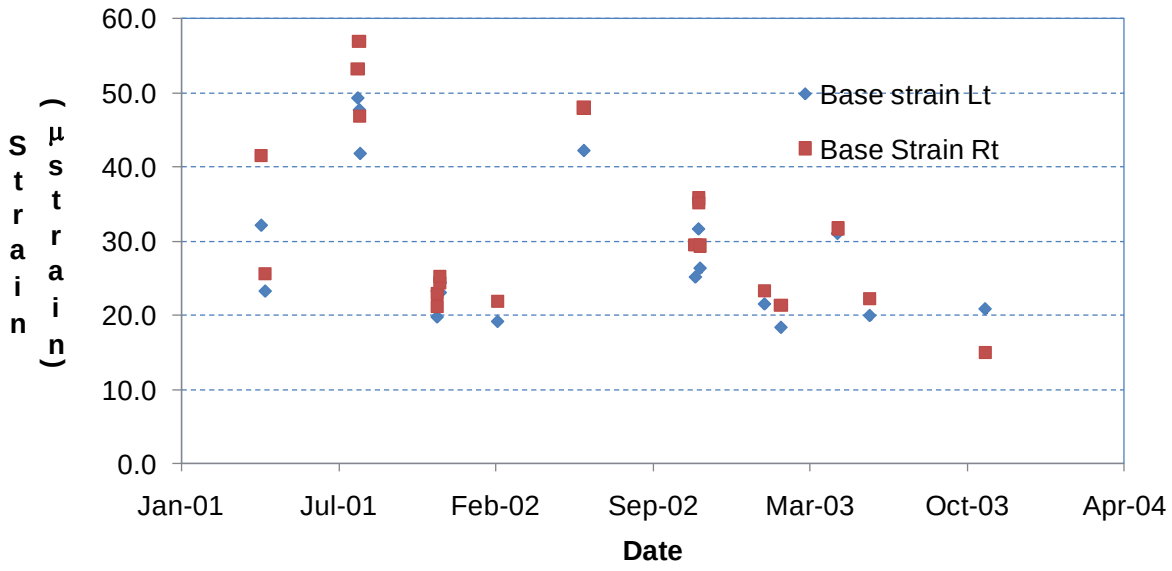


**(b) Experiment III**

**Figure 15**
**Longitudinal strain measurements at the bottom of the HMA layers (3.5 in.)**

**Seasonal and Thermal Variations**

Due to the viscoelastic nature of HMA, significant variation in the response is expected with the change in temperature. While other seasonal factors such as moisture may have an impact on the measured response, it is assumed that adequate drainage conditions were predominant at the site. Temperature measurements were not conducted in the pavement structure during the testing process. However, ambient air temperatures for the exact date and time reported in the instrumentation files were obtained for the Port Allen weather station from the National Climatic Data Center through the following website: http://lwf.ncdc.noaa.gov/oa/ncdc.html. Figure 16(a) illustrates the change in the measured strain in Experiment II at the bottom of the surface layers (3.5 in.) with the change in temperature for the first load level (i.e., up to 400,000 passes). Similarly, Figure 16(b) illustrates the change in the measured strain in Experiment III at the bottom of the HMA layers (3.5 in.) with the change in temperature for the first load level (i.e., up to 200,000 passes).

As shown in Figure 16 (a and b), one may assume that pavement strain varies exponentially with temperature, which would be in agreement with the findings of previous research studies *[5], [30]*. While the measured strain was influenced by the change in temperature, it expected that other factors such as change in measurement conditions and materials' damage need to be considered to thoroughly explain change in strain throughout the experiment. These factors are discussed further in the subsequent sections of this report.

Figure 17(a) illustrates the variation of the measured strain in the early stage of Experiment III (up to 50,000 passes). In this stage, minimal change is expected in the pavement and measurement conditions. As shown in this figure, an exponential regression line similar to the one shown in Figure 16(a) may be used to fit the data. To level the effect of temperature from the measurements, this regression model was used to determine the response at a reference temperature of 25°C using correction factors determined from the following model:

$$CF = e^{0.0669(T-25)} \qquad R^2 = 0.86 \qquad (6)$$

where,

CF = correction factor to shift measured strain from a temperature T to a reference temperature of 25°C.

Similarly, the following model was used to shift the strain measurements to a reference temperature of 25°C in Experiment II, Figure 17(b):

$$CF = e^{0.053(T-25)} \qquad R^2 = 0.92 \qquad (7)$$

where,

CF = correction factor to shift measured strain from a temperature T to a reference temperature of 25°C.

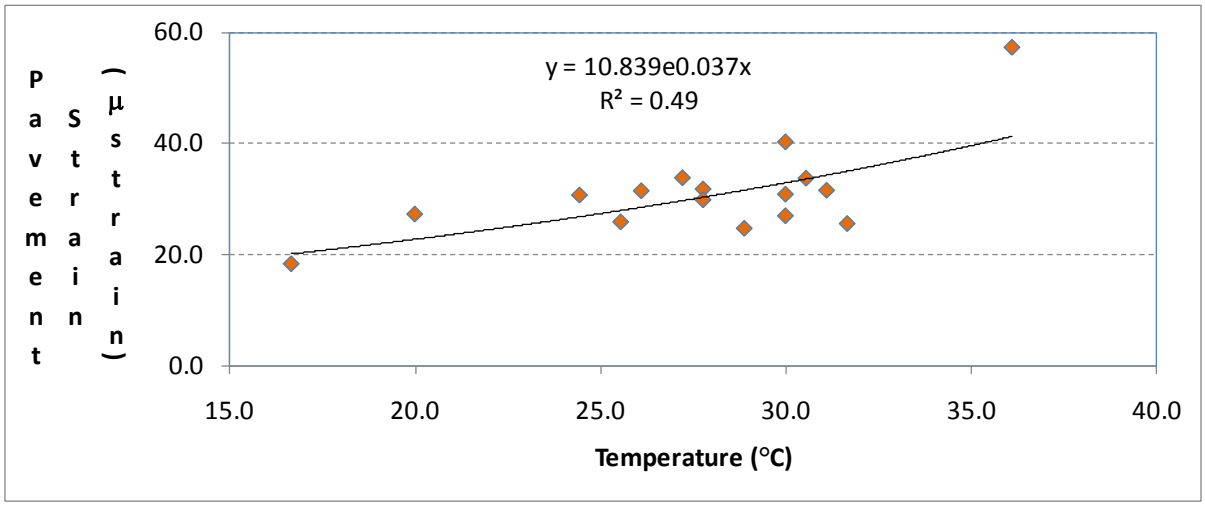


**(a)**

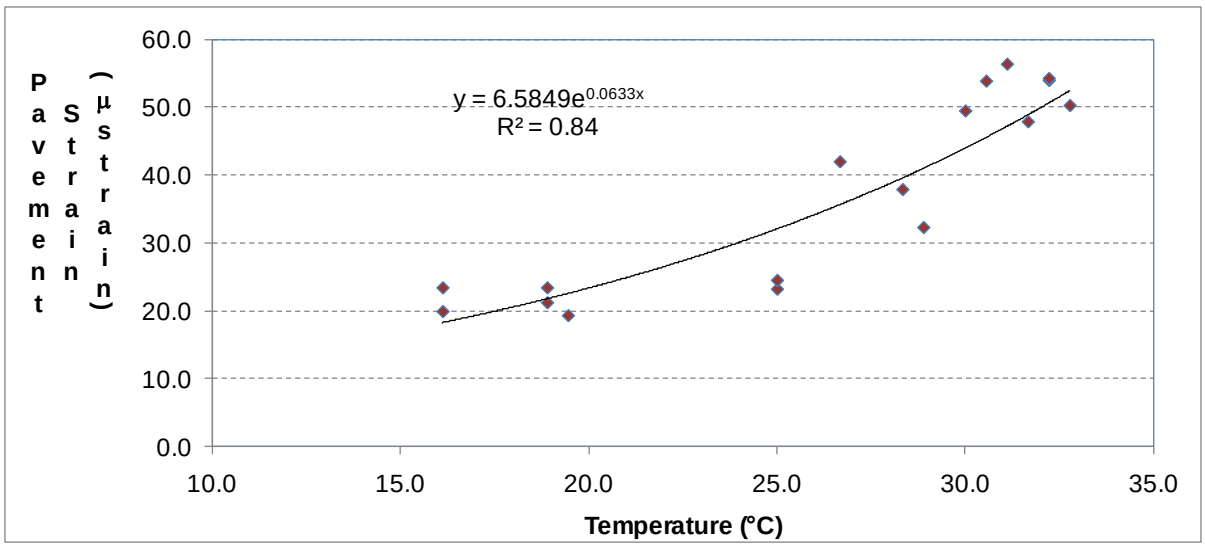


**(b)**

**Figure 16**
**Variation of the longitudinal strain (depth = 3.5 in.) with ambient air temperature in (a) Experiment II and (b) Experiment III**

Figure 18(a) presents the change in the measured vertical stress at the bottom of the HMA layers as a function of temperature (Experiment III). As shown in this figure, measured stress was also found to vary exponentially with the change in temperature. However, this trend was not validated in Experiment II, which seemed to indicate that the measured stress was independent from the change in temperature, Figure 18(b). Based on the results shown in Figure 18(a), a regression model was developed to shift the measured stress to a reference temperature of 25°C in Experiment III:

$$CF = e^{0.0344(T-25)} \qquad R^2 = 0.99 \qquad (8)$$

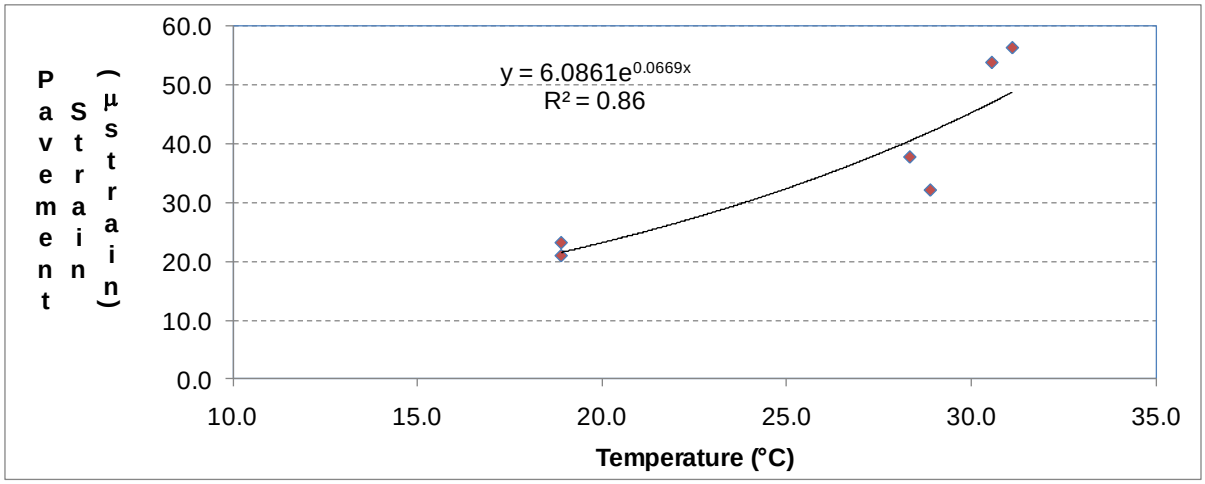


**(a)**

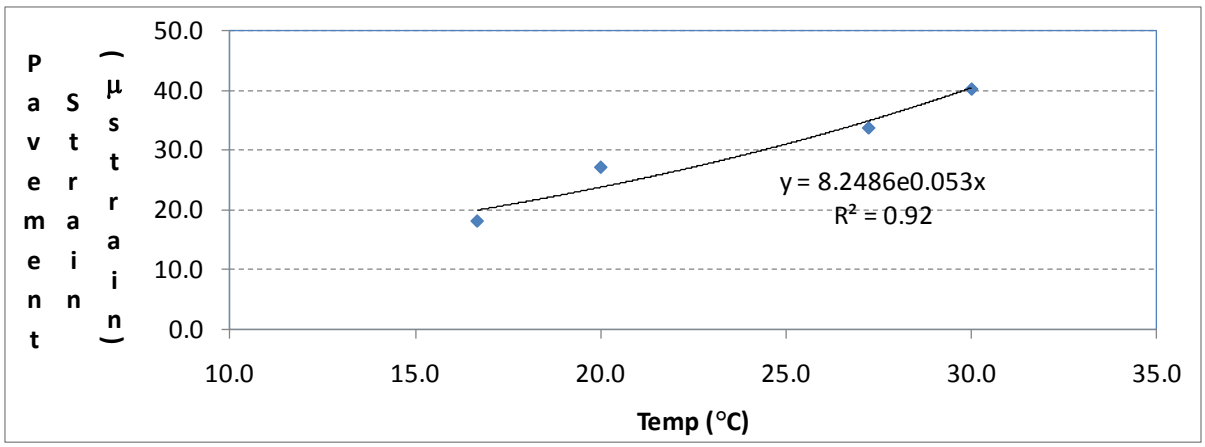


**(b)**

**Figure 17**
**Variation of the longitudinal strain with temperature in the early loading stage in (a) Experiment III and (b) Experiment II**

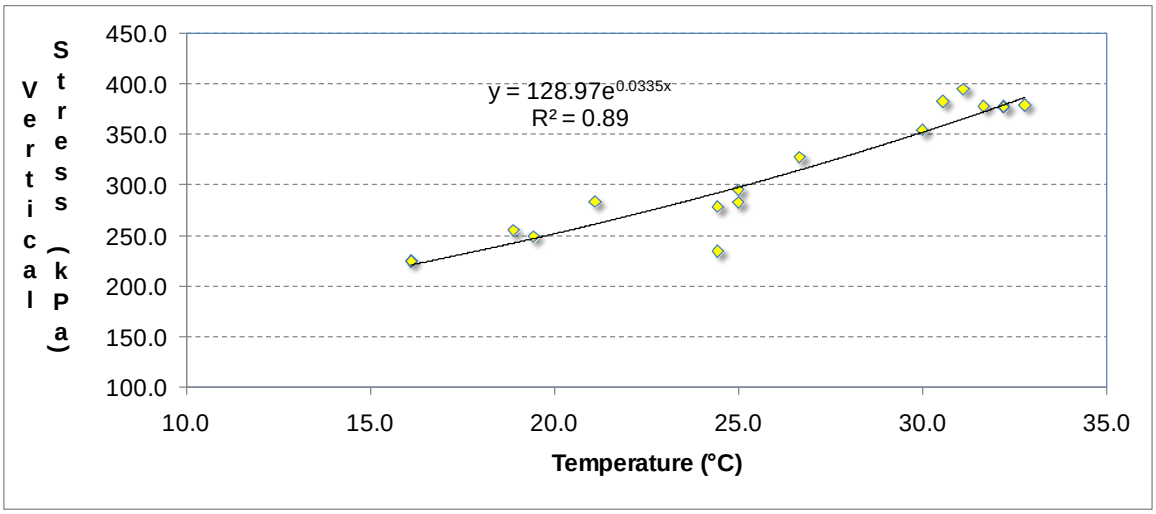


**(a)**

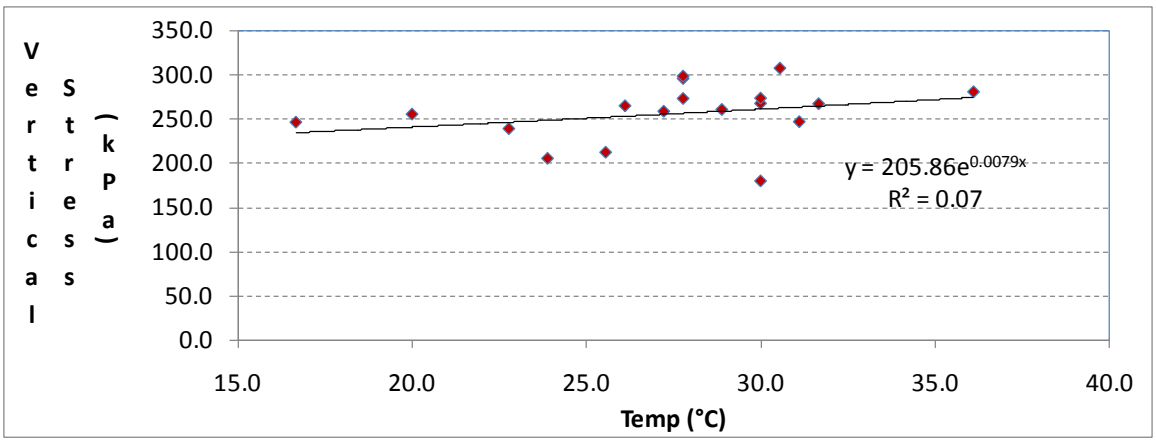


**(b)**

**Figure 18**
**Variation of vertical stress with ambient temperature in (a) Experiment III and (b) Experiment II**

**Evolution of Pavement Damage**

Based on equations (6) and (7), measured strain responses were shifted to a reference temperature of 25°C. Shifting of the measurements allowed characterizing the effect of pavement damage without confounding it with the effect of temperature. Figure 19(a) illustrates the variation of the temperature-corrected strain at the bottom of the HMA layers in Experiment III with the number of passes. Similarly, Figure 19(b) presents the variation of the temperature-corrected strain at the bottom of the HMA layers in Experiment II with the number of passes. As shown in Figure 19(a), the measured strain increased slightly at the beginning of the experiment but then decreased progressively with the increase in number of passes. After the second load level was applied, an increase in strain was noted followed by a gradual decrease in the response. A similar trend was noted in Experiment II as shown in Figure 19(b). As shown in this figure, an increase in strain was noted after the increase in load followed by a gradual decrease in the response.

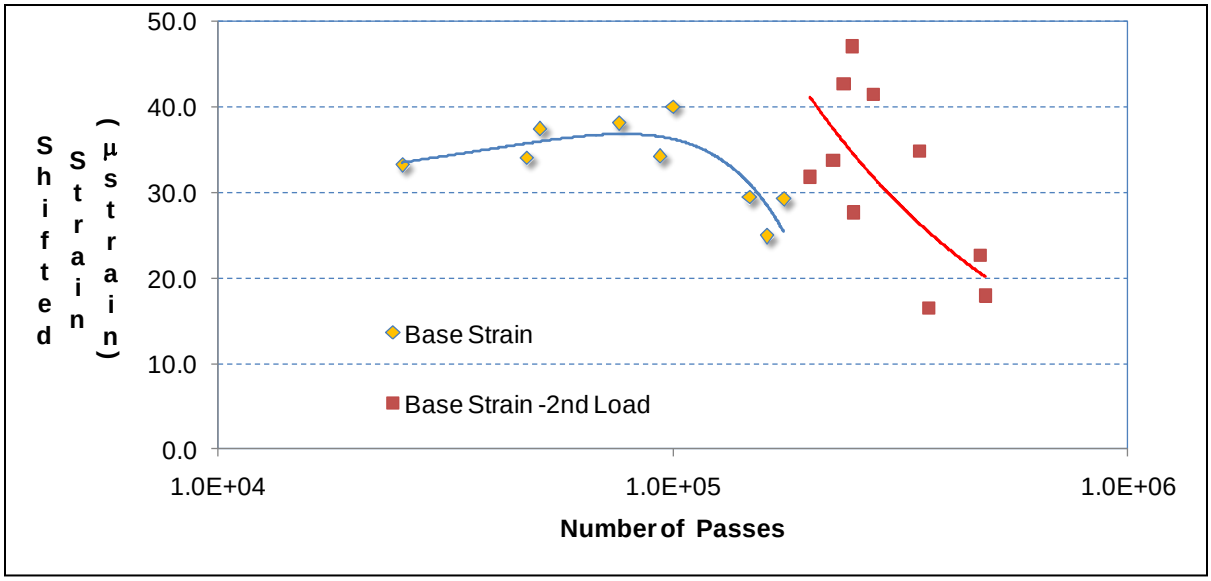


**(a)**

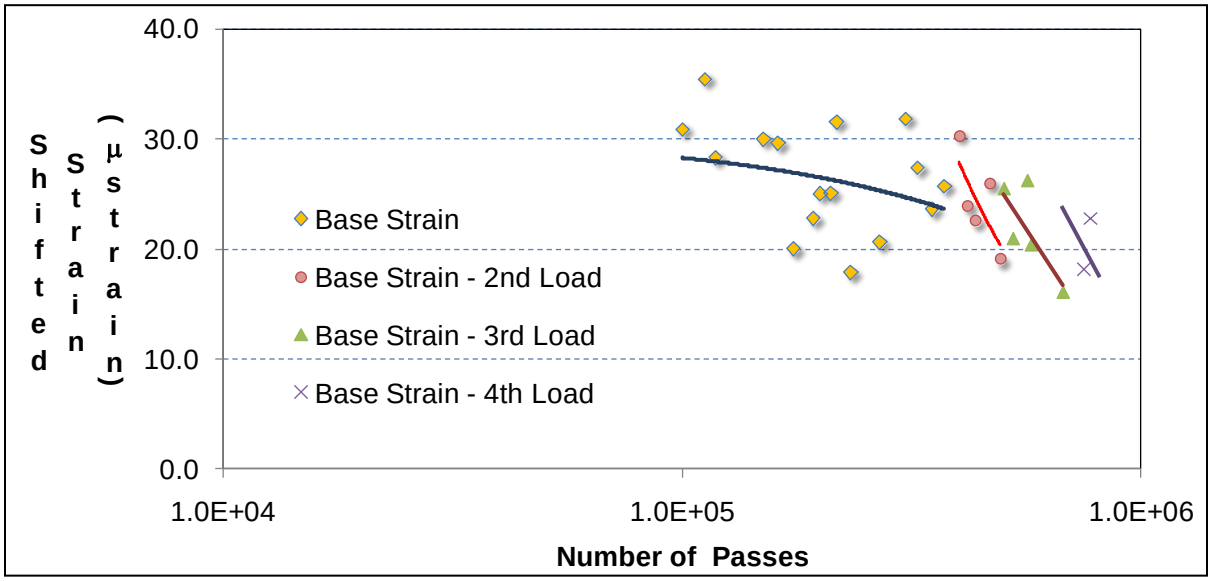


**(b)**

**Figure 19**
**Variation of the temperature-corrected longitudinal strain with number of passes in (a) Experiment III and (b) Experiment II**

Although it is expected that with the increase in pavement damage, the measured strain should gradually increase, an indication of material weakening; however, a reversed trend was observed. This hypothesis is supported by the results presented in Figure 20, which shows that the backcalculated HMA moduli from falling weight deflectometer (FWD) testing decreased continuously throughout Experiment III indicating progressive damage of the material. These FWD tests were conducted at a relatively uniform temperature ranging from

38 to 45°C; therefore, no temperature correction was applied on the backcalculated moduli. It is worth noting that a recent research study concluded that strain measurements taken at the surface were also not a good indicator of damage development *[32]*. It appears that with the increase in number of passes, the strain gages dispersed the material around them resulting in less contact with the surrounding medium and, therefore, a smaller strain was measured.

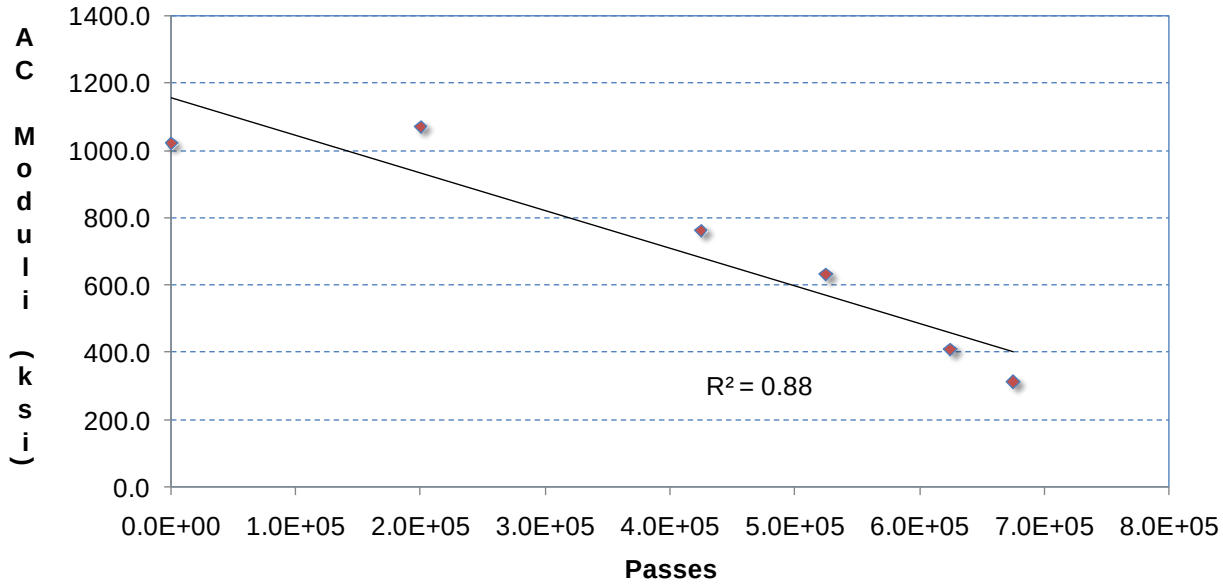


**Figure 20**
**Variation of backcalculated HMA moduli with the increase in number of passes in Experiment III**

Figure 21 presents the variation of the temperature-shifted vertical stress with the number of passes in Experiment III. As shown in this figure, measured vertical stress remained fairly constant with the increase in number of passes during the first load level. After the second load level was applied, an increase in vertical stress occurred, followed by a fairly constant response. As it was previously noted, responses of the gage after 250,000 passes were not used in the analysis. This behavior was expected since the stress applied on the material mainly depends on the magnitude of the external load and not on the level of damage in the material.

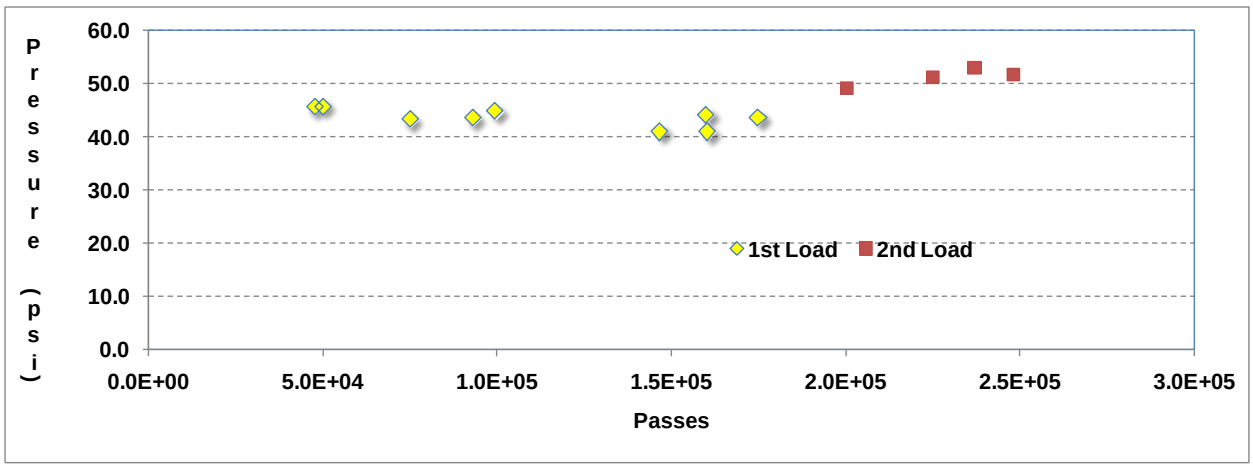


**Figure 21**
**Variation of the vertical stress at the bottom of the HMA layers with the number of passes in Experiment III**

**Recommended Modifications to the Instrumentation Strategy in Future Experiments**

Based on the analysis conducted in this study, a number of modifications to past instrumentation strategies are recommended. Specifically, the following course of actions is recommended:

(1) Measurements should be intensified in the early stage of the experiment as these responses are usually very valuable to compare different pavement technologies and for validation of theoretical models. It is recommended that continuous measurements be conducted for the first 100,000 passes (e.g., every 1,000 passes).
(2) Temperature sensors such as thermocouples should be installed in future experiments. These sensors are relatively inexpensive and their readings are critical in order to assess seasonal and thermal variations in the pavement system.
(3) Adopted gages in past experiments seem to provide acceptable durability as compared to other pavement gages. However, long-term monitoring of pavement damage does not seem possible with current sensor technologies. A new class of fiber optic strain gages has been recently introduced to monitor strain responses in HMA and may be tested in future experiments *[33]*. These sensors permit measurement of static and dynamic pavement responses and were reported to provide reliable measurements with little or no noise and to allow for long-lasting strain monitoring *[34]*.
(4) Since pressure cells in granular layers seem to tilt during construction or just after the loading starts, compaction of the supportive layer for these cells needs to be improved in future experiments.

(5) Distance between the sensors needs to be increased in the longitudinal direction from 1.2 ft. to at least 1.6 ft. This will prevent interference between the different gages as they tend to act as reinforcement to the pavement system; see Figure 22. As shown in this figure, instruments located at the same depth are staggered to increase the distance between them.

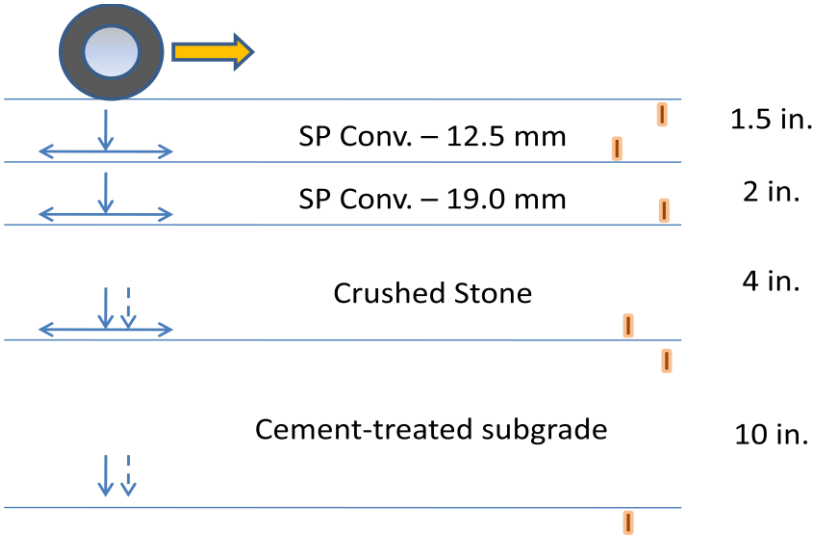


**(a)**

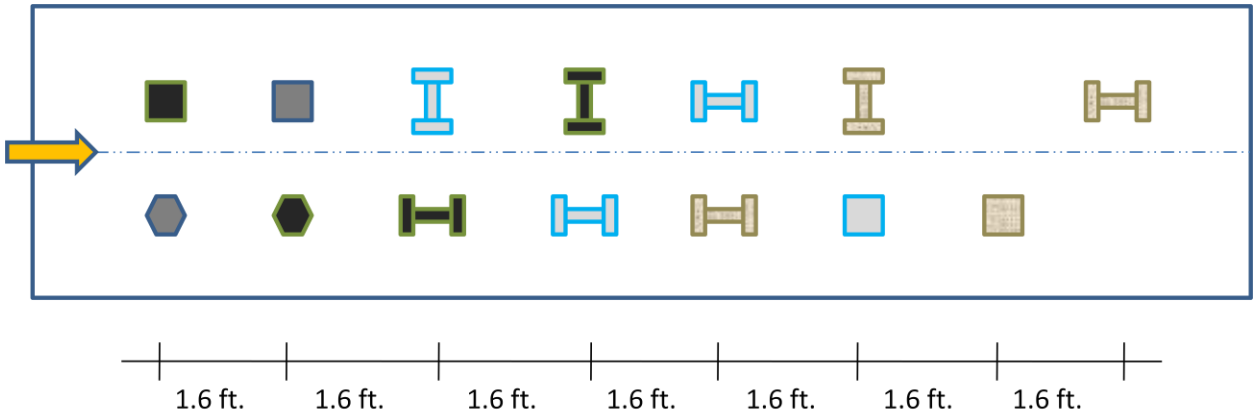


**(b)**

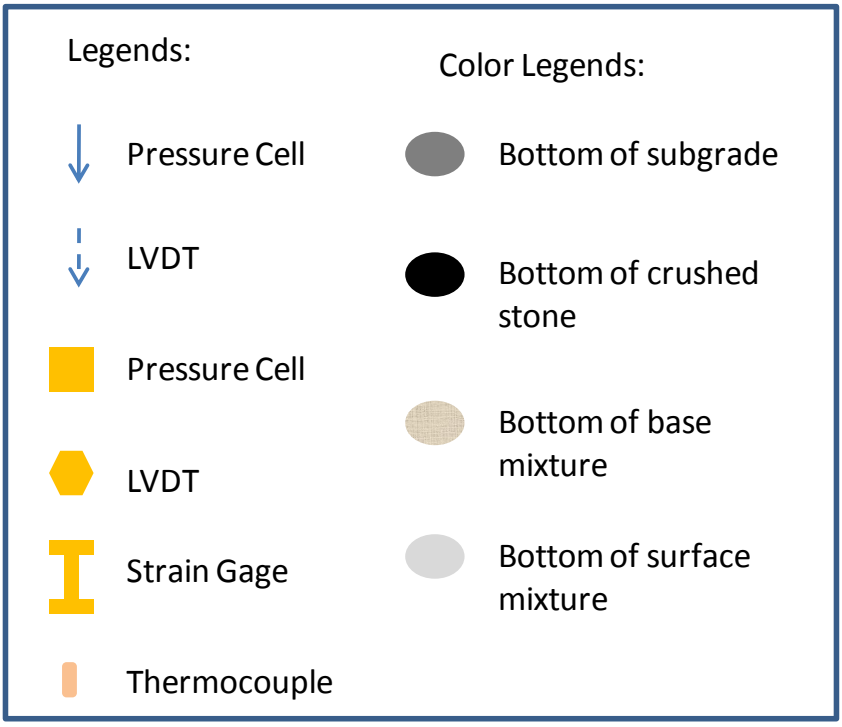


**(c)**

**Figure 22**
**Proposed instrumentation strategy for one of the six test lanes proposed in Future ALF Experiment V**

(6) The use of linear-variable differential transducers (LVDT) in the granular layers is recommended to allow for measuring vertical deflection in unbounded materials. In addition, monitoring strain in the HMA layers may be beneficial in both the longitudinal and transverse directions.

(7) While the use of cement-treated base and subgrade materials has been beneficial to Louisiana, the use of cement-stabilized materials at the ALF facility does not seem beneficial or cost-effective. The use of this pavement material extends the experiment over a long period of time that may not be necessary. Instead, it is recommended to avoid this layer in future designs at the ALF facility as most of the research is focused on upper HMA layers. Avoiding cement-treated materials will allow determining the relative performance of different pavement technologies in a cost- and time-effective manner.

## Analysis of Laboratory Test Results

Figure 23 shows the relationship between the measured ductility and the failure strain measured using the direct tensile test (DTT). Each binder was tested in four replicates using the ductility test and six replicates using the DTT. The average coefficient of variation for DTT measurements (PAV-residues) was 19 percent while it was 4 percent for the ductility test (RTFO and PAV-residues). As shown in this figure, there was an inverse correlation between binder ductility at 25°C and the measured failure strain at -12°C. In other words, a binder that provides high ductility at 25°C would be characterized by poor elongation properties at low temperature (-12°C). It also appears that while three binders would pass the ductility criterion specified by Louisiana (binders G, H, and I), these binders will not pass or barely pass the Superpave DTT criterion of a minimum of 1 percent failure strain. However, since the DTT is only used as a referee test, these binders would still be classified as PG 64-22 since they satisfy the BBR stiffness criterion (Table 2).

These results indicate that the current Superpave specifications fail to differentiate between these binders in terms of performance since they may all be used as PG 64-22 binders and are expected to exhibit similar pavement performance. Since past research has widely established the relation between asphalt ductility and pavement performance, it would be expected that these binders would not exhibit the same performance in the field *[12], [13]*.

To explain the results presented in Figure 23, this study laid out two hypotheses that may be used to rationalize the observed rheological behavior and to provide insight into the relationship between molecular compositions of the binder and its physical properties:

(1) Effect of aging: while the ductility test is performed on RTFO-binder residue, the direct tensile test uses PAV-binder residue. High-ductility binders may experience greater loss of light components than low-ductility binders during the aging process, and therefore, exhibit a brittle behavior at low temperatures.
(2) Effect of temperature: while ductile binders may perform satisfactorily at intermediate temperature, some of the tested binders may experience a greater rate of crystallization at low temperatures, and therefore, exhibit a brittle behavior during the DTT.

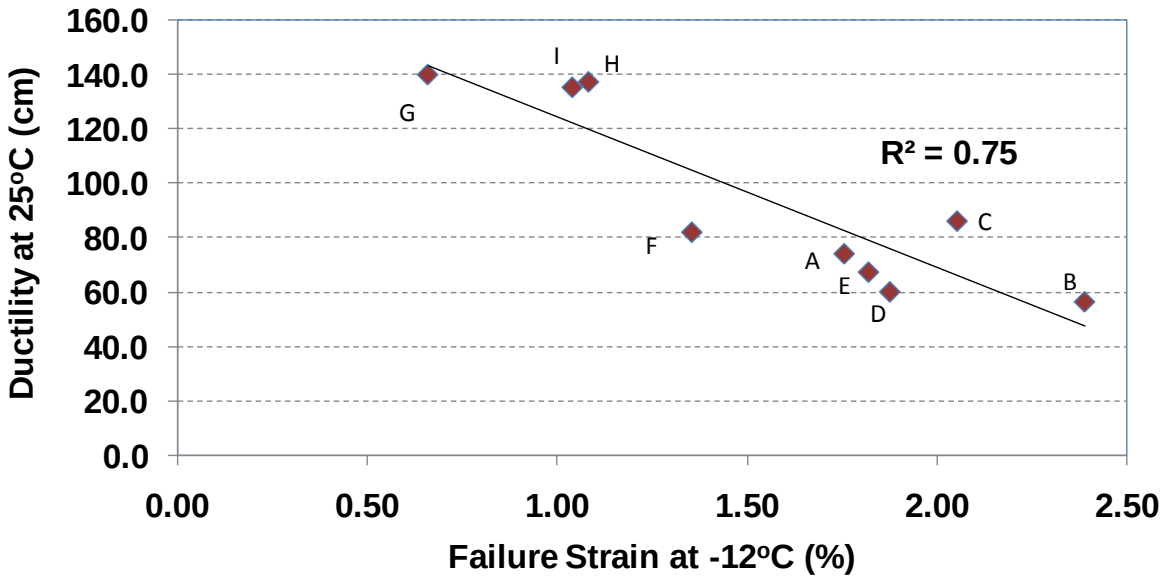


**Figure 23**
**Relationship between measured binder ductility (RTFO-aged) and failure strain from DTT (PAV-aged)**

**Effect of Aging**

While the ductility test is conducted on RTFO-aged binders for specification purposes, the same test was performed on PAV-aged binders. This allowed comparing results of the direct tensile test to the ductility test under the same aging conditions. Figure 24 presents the relationship between the measured binder ductility and the failure strain from the direct tensile test for PAV-aged binder residues. As shown in this figure, an inverse correlation between the binder ductility and the measured failure strain was still observed indicating that the aging process is not the main factor causing this reverse trend.

These findings were supported by the results of HP-GPC tests. Figure 25 (a and b) present the fractional compositions of the tested binders in the original and PAV-aged conditions, respectively. The composition of the binders are divided into three main categories: medium molecular weight (MMW), which represents the percentage of asphaltenes in the binder; low molecular weight (LMW), which represents the percentage of paraffinic maltenes in the binder; and others, which represent the percentage of very light oils in the binder. While the asphaltenes component is generally hard, brittle and, non-elastic, the maltenes component is soft, flexible, and elastic.

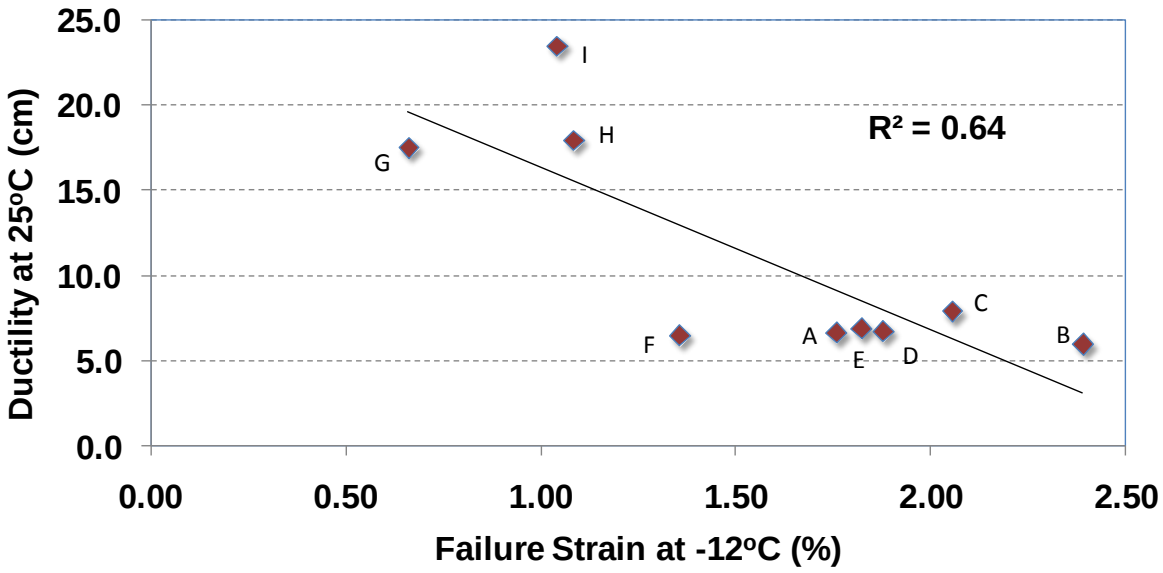


**Figure 24**
**Relationship between measured binder ductility (PAV-aged) and failure strain from DTT (PAV-aged)**

The relationship between binder molecular compositions and its rheological behavior is evident by comparing the molecular compositions of binders G and I (the most ductile binders) to binders D and E (the least ductile binders). As shown in Figure 25 (a and b), binders G and I had a high percentage of maltenes (82.9 and 84.1% in the original state and 80.7 and 79.4% after PAV aging) while binders D and E had a low percentage of maltenes (78.8 and 77.4% in the original state and 76.5 and 75.6% after PAV aging). This implies that at the same temperature, a straight binder that is characterized with high ductility before aging would also be characterized by good extensibility properties after aging. This explains why a similar trend was observed in Figures 23 and 24 and confirms that aging is not the controlling factor for this reverse trend. It is also interesting to notice that the first seven binders, which originated from the same crude oil source, seem to lose about 2 percent of low molecular weight components in the aging process.

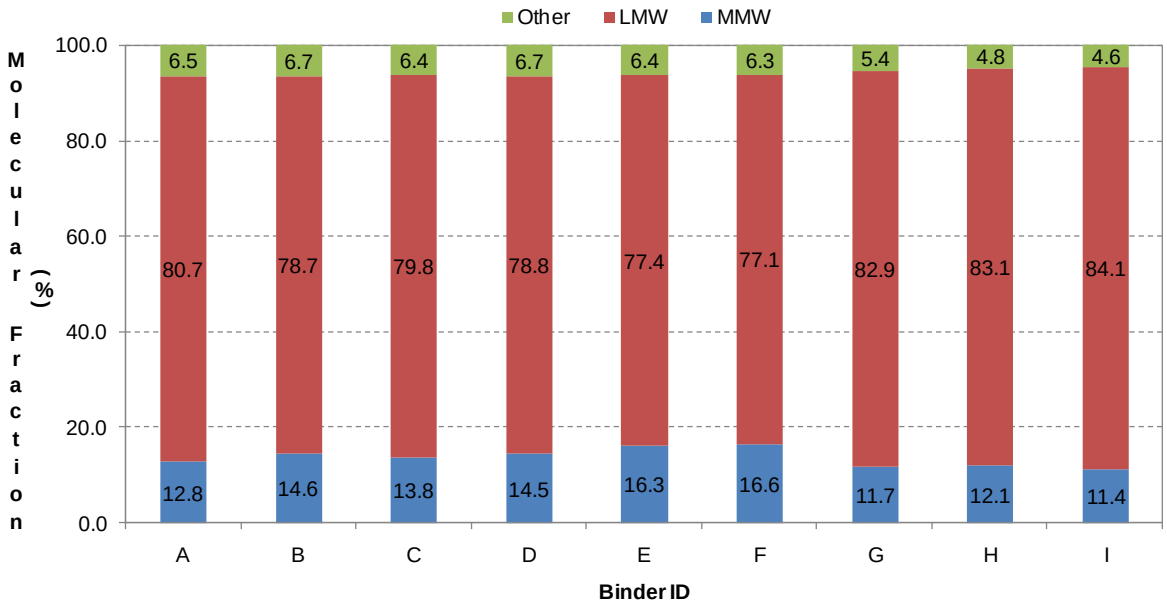


**(a)**

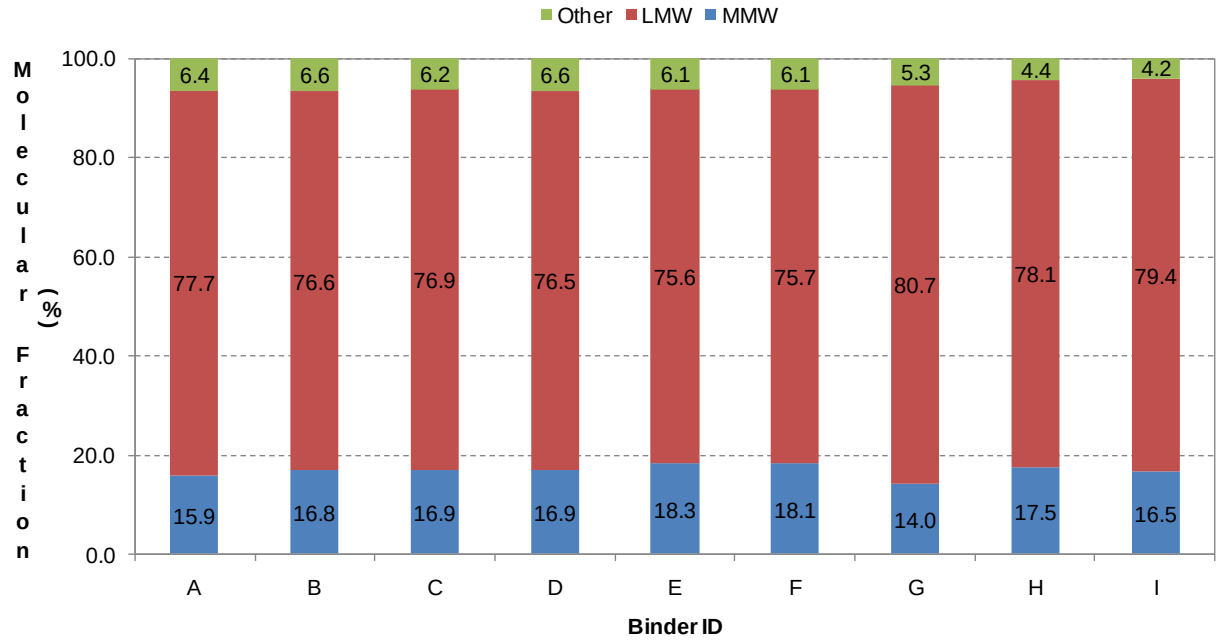


**(b)**

**Figure 25**
**Molecular fractional distributions for (a) original binders and (b) PAV-aged binders**

**Effect of Temperature**

Three asphalt binders were selected for laboratory characterization using differential scanning calorimetry and dynamic mechanical analysis. The selected asphalt binders exhibited contrasting rheological behaviors: low ductility (25°C) and low stiffness (-12°C) (asphalt binder D) and high ductility at intermediate temperature and high stiffness at low temperature (asphalt binders G and I). A typical modulated DSC curve is shown in Figure 26 for binder G (original). This curve can be used to calculate enthalpies of transitions by integrating the peak corresponding to a given transition and to determine crystallization events at a given temperature. This information is very valuable since the percentage of crystallizable species is an indicator of brittle behavior at a given temperature. The DSC content of crystallizable species was determined below and above 25°C by referring the enthalpy of sample melting (determined as an endothermic transition on the heat flow plot) to the melting enthalpy of 100% crystalline polyethylene (293 J/g) and the content of LMW fractions (maltenes) previously determined from GPC.

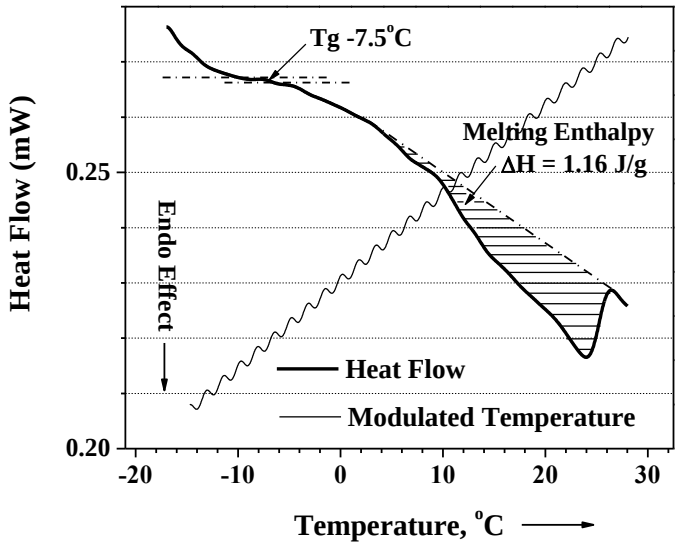


**Figure 26**
**Modulated DSC analysis of asphalt binder G (original)**

The glass transition temperature of the selected binders was determined using DMA. The glass transition temperature is identified by the temperature at which E" peaks when plotted against the test temperature. A typical example of this plot is presented Figures 27 and 28 for binders G (RTFO-residue) and I (PAV-residue), respectively. In all tested cases, the sample broke right after passing the glass transition temperature confirming that the material is behaving similar to a crystalline-brittle solid.

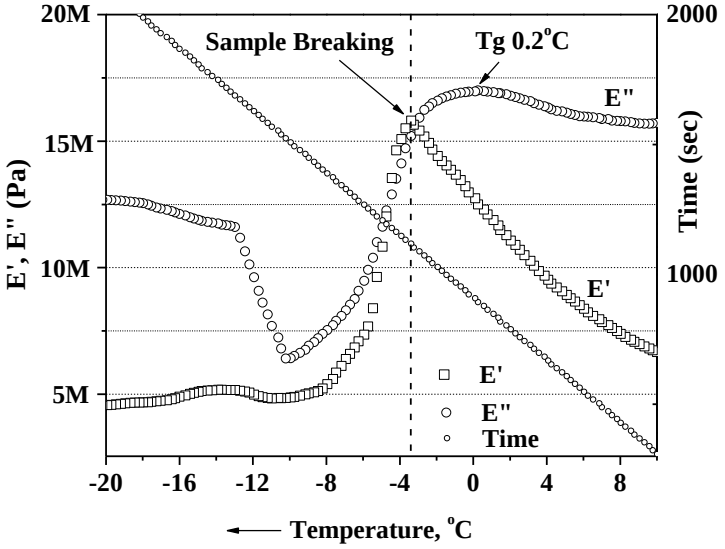


**Figure 27**
**DMA of asphalt G (RTFO-residue) showing the sample breaking just below the glass transition temperature (E' is the storage modulus, and E" is the loss modulus)**

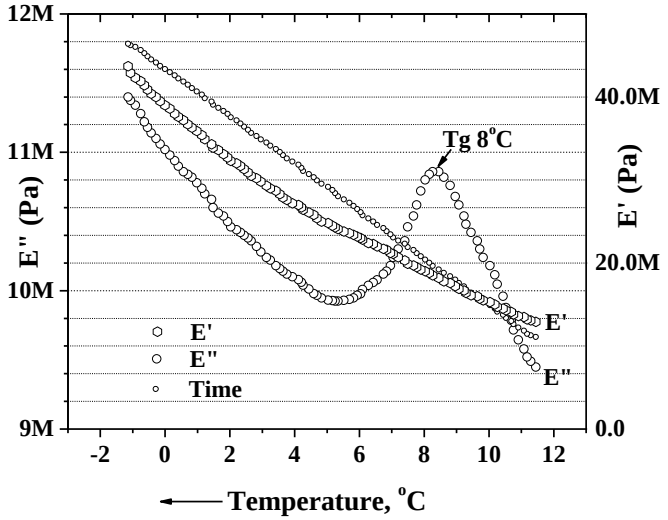


**Figure 28**
**Glass transition temperature (DMA) of binder I (PAV-residue)**

The content of crystallizable species of selected asphalt binders determined by DSC is presented with the glass transition temperature determined by DMA in Table 4. The crystalline fractions melting above 25°C presented in this table have an adverse effect on the sample ductility at intermediate temperature since these fractions act as brittle components.

The ductility of asphalt binder D, lower than that of binders G and I, may be explained by its higher content of crystalline fractions melting above 25°C (Table 4). On the other hand, the crystalline fractions melting below 25°C may have a negative effect on the sample stiffness at low temperature. This is the case of asphalt binder G (PAV-residue) with 0.86% LMW crystalline fractions melting below 25°C, which was higher than for asphalt binder D in which no melting of crystalline species has been detected in the same temperature range. However, the stiffening of asphalt binders at low temperatures is a complex phenomenon in which paraffinic (maltene) crystallization might only have a reduced role. This is evident by the results of DSC analysis for binder I, which had a very small content of LMW crystalline fractions but still showed poor elongation properties at low temperature.

**Table 4**
**Glass transition (DMA) and the content of crystallizable species (DSC) of asphalt binders**

| Asphalt Binder | Glass Transition Tg (˚C) | Crystallizable Species Below 25°C (%)* | Crystallizable Species Above 25˚C (%)* |
|---|---|---|---|
| D original | -4.5 | Not detected | 0.18 |
| D RTFO | -3.3 | Not detected | 0.41 |
| D PAV | 3.5 | Not detected | 0.37 |
| G original | -7.5^ | 0.48 | 0.12 |
| G RTFO | 0.2 | 0.41 | 0.33 |
| G PAV | 7.4 | 0.86 | Not detected |
| I original | 5.0 | 0.03 | 0.12 |
| I PAV | 8.3 | Not detected | 0.10 |

* As a percentage of maltene fractions; ^ determined from DSC

In the glassy state, amorphous components will act as rigid, stiff, and brittle molecular fractions and may cause the binder to exhibit poor extensibility and high stiffness. Results of DMA showed that asphalt binders characterized by high stiffness and poor extensibility at low temperature have a higher $T_g$ than that of low stiffness binders. As shown in Table 4, the glass transition temperatures for asphalt binders G-PAV and I-PAV (7.4 and 8.3°C, respectively) were higher than that of low stiffness asphalt binder D (3.5°C). The glass transition temperature of binder G in the RTFO state was also higher than the one for binder D in the same aging state.

**Relationship between Molecular Compositions and Binder Physical Properties**

While molecular composition of asphalt binder is not specified by state highway agencies, it would be beneficial to determine whether performance of the binder can be correlated to its chemical constituents. Figure 29 shows the relationship between the percentage of low

molecular weight in the binder and the rutting criterion currently used in the Superpave specification system (G*/sinδ). As shown in this figure, a positive correlation exists between the percentage of LMW in the binder and its rutting resistance as predicted by the criterion of G*/sinδ for the original binder. Such correlation has also been reported for crumb rubber–modified binders and is supported by the results presented in this figure for unmodified straight binders *[35]*. This referred study also found that adding a rejuvenating agent to the binder decreases the content of LMW in the binder and, therefore, results in a decrease in the binder rutting resistance.

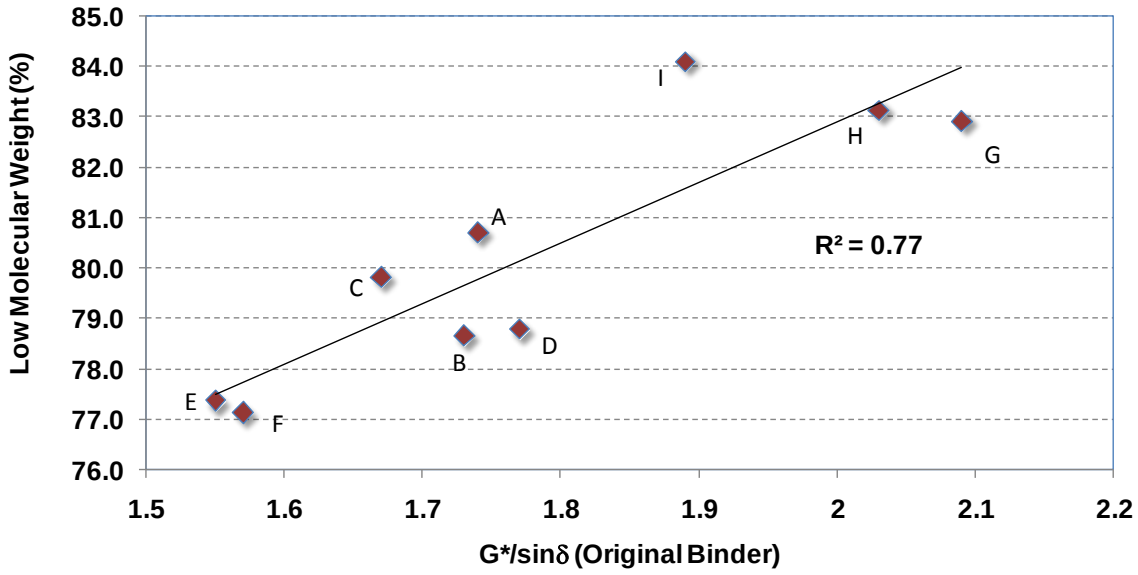


**Figure 29**
**Relationship between percentage of low molecular weight and binder resistanceto rutting**

As previously noted, the binder content of low molecular weight was also found to correlate positively with its ductility at intermediate temperature. In other words, an increase in the binder content of LMW results in an increase in its ductility at intermediate temperature. Results presented in Figure 30 also indicate that the increase in LMW results in an increase in the binder stiffness at low temperature as measured by the Bending Beam Rheometer (BBR) at -12$^{o}$C. As it was previously noted, an increase in paraffinic maltene content results in some of the light components to crystallize at higher temperatures as it approaches the glassy region. Therefore, an increase in LMW indicates that the binder would behave as a brittle material at low temperatures and would be more susceptible to thermal cracking. However, one should acknowledge that this correlation may not hold true for all crude oil sources and some amorphous maltene components may not crystallize at low temperatures

providing the user with optimum behavior (high elongation) at both intermediate and low temperatures.

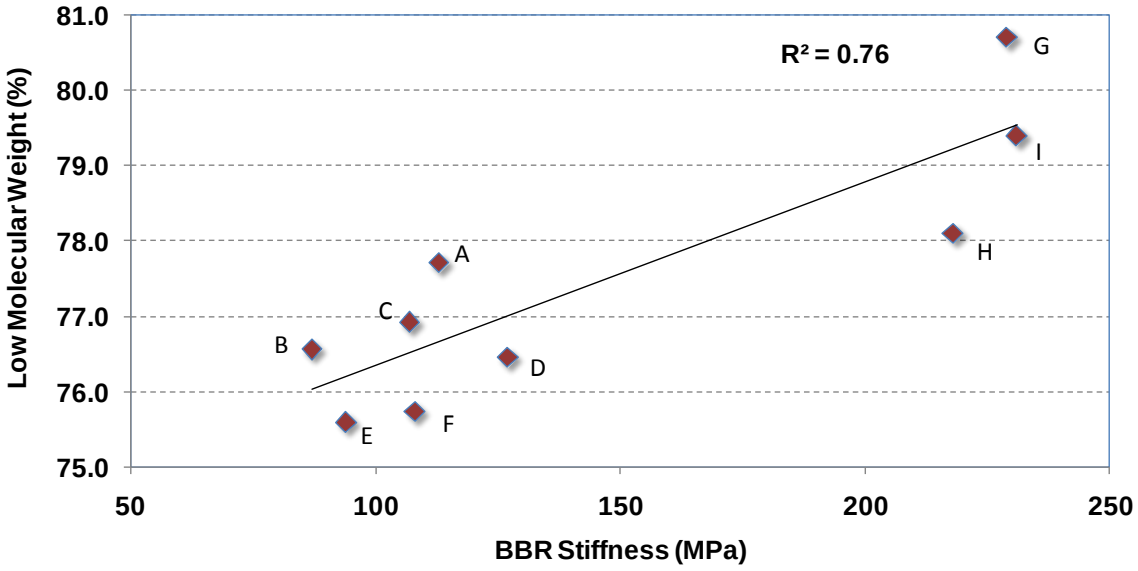


**Figure 30**
**Relationship between percentage of low molecular weight and binder stiffness at low temperature**

**Relationship between Binder Ductility and Mixture Performance**

The previous results clearly established the differences between the tested binders in terms of ductility, tensile strain at failure, and molecular compositions. However, one may not conclude whether the noted differences would have an impact on the mixture performance and whether the measured binder rheological properties have a significant effect on the mix performance. It is noted that all binders were classified as PG 64-22 binders and are, therefore, expected to exhibit similar mix performance according to the Superpave binder specification system. However, past research has shown that asphalt ductility has a significant effect on mix performance *[12], [13]*. To answer this critical question, three binders (B, F, and G) with contrasting levels of ductility were selected and were used to prepare asphalt mixes according to the mix design developed by Mohammad et al. *[27]*. These samples were then tested using the ITS Test.

Figure 31 (a and b) presents the variation of the ITS with the binder ductility in the unaged and aged conditions. The values shown in these figures are the averages of three samples with a coefficient of variation ranging from 6 to 9 percent. As shown in these figures, there was a clear relationship between the binder ductility and the measured tensile strength of the

mixture. In other words, using a binder with a high ductility resulted in a mixture with greater indirect tensile strength.

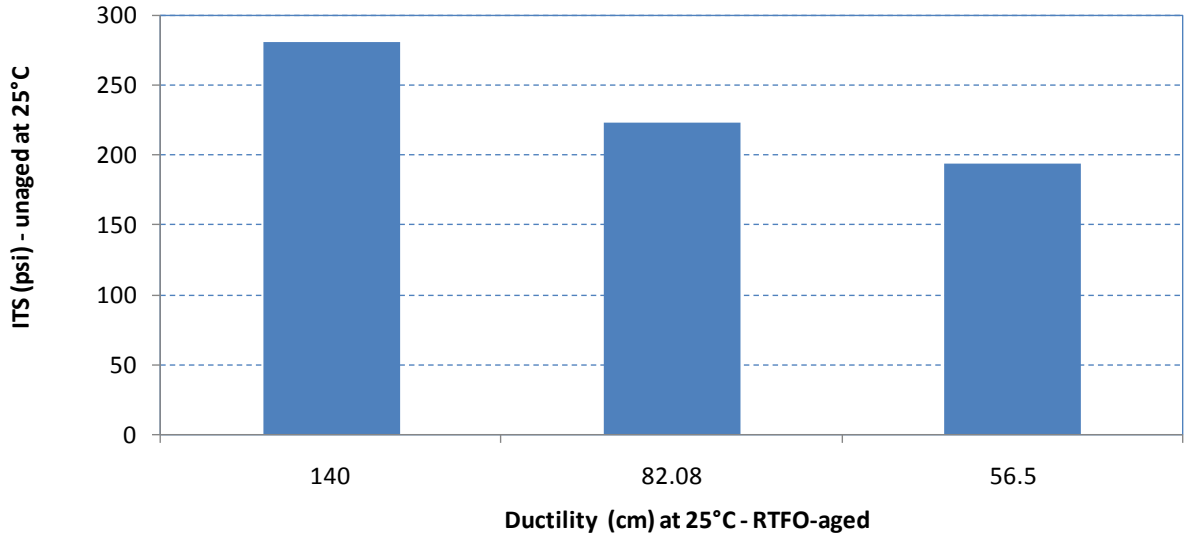


**(a)**

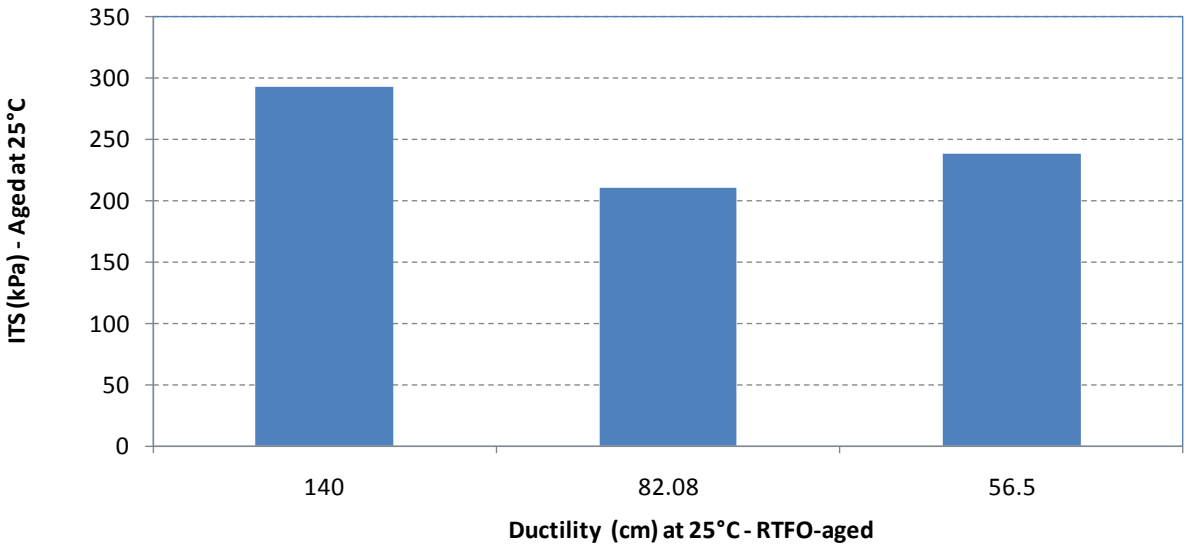


**(b)**

**Figure 31**
**Relationship between the mixture indirect tensile strength and the binder ductility**

Figure 32 (a and b) presents the variation of the tensile strain at failure with the binder ductility in the unaged and aged conditions. As shown in these figures, a binder with high ductility was associated with high tensile strain at failure. As it was previously noted, asphalt

mixtures with high strain at failure were found to resist cracking better than mixtures that were more brittle with low tensile strain at failure *[21]*.

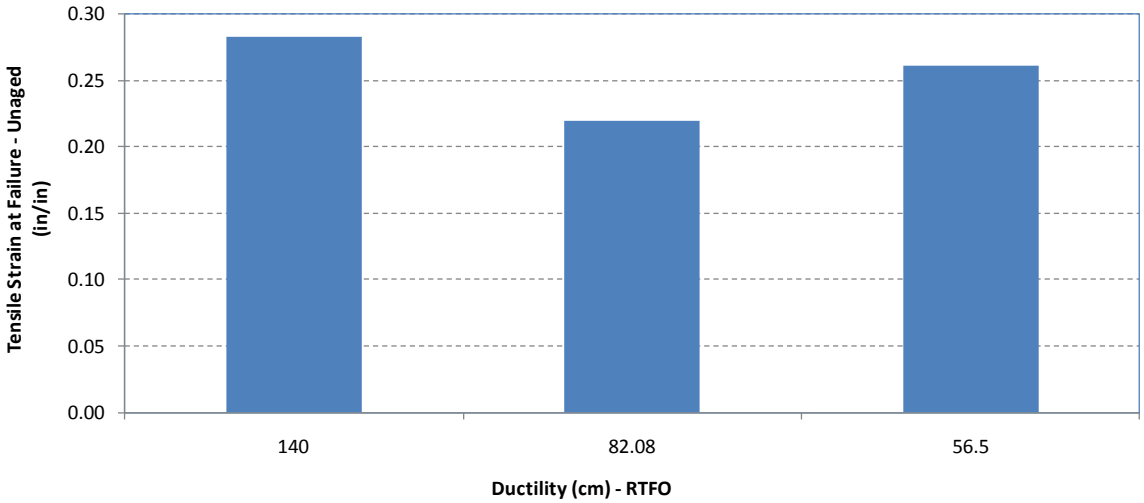


**(a)**

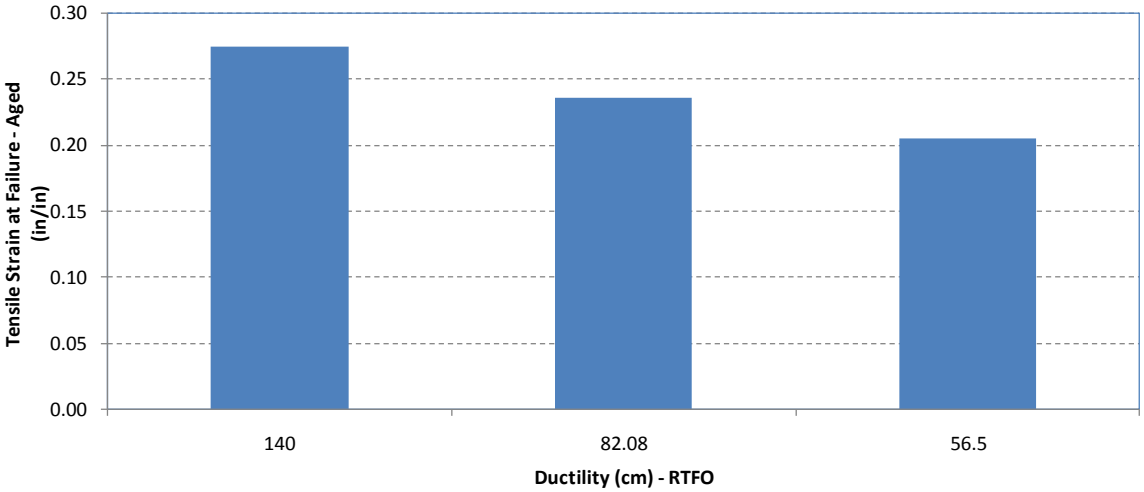


**(b)**

**Figure 32**
**Relationship between the mixture tensile strain at failure and the binder ductility**

**Relationship between Binder Ductility and the Multiple Stress Creep Recovery Test**

Linearity tests were conducted on the selected binders in order to determine suitable stress levels that would lie in the linear viscoelastic region at 25°C. The linear region was defined as the region starting from the beginning of the test until the complex shear modulus falls to 95% of its original value. Based on this definition, two stress levels of 20 kPa and 40 kPa were selected to be in the linear viscoelastic region at 25°C. Three binders (B, F, and G) with contrasting levels of ductility were then evaluated using the MSCR test. Figure 33 (a

and b) presents the relationship between the binder ductility and the percentage recovery and the non-recoverable creep compliance, respectively. The recovery and non-recoverable creep compliance shown in this figure is the average of six samples conducted at two stress levels. The average coefficient of variation between three samples conducted at the same stress level was 1 percent for the percentage recovery and 10 percent for the non-recoverable creep compliance.

As shown in this figure, there was an inverse relationship between binder ductility and percentage recovery in the MSCR test. Moreover, a binder with high ductility would be characterized by high non-recoverable creep compliance. This means that a binder characterized with a high level of ductility would exhibit poor performance in the MSCR test. It is not clear why an inverse relationship was found between these tests parameters, and an in-depth evaluation of these findings should be conducted in the future. However, one may hypothesize that this difference is related to the fact that the ductility test is conducted to failure while the MSCR test is conducted at a low level of stress in the linear viscoelastic region. It is recommended that future research conduct the MSCR test at a high stress level that would induce damaging non-recoverable deformation in the binder.

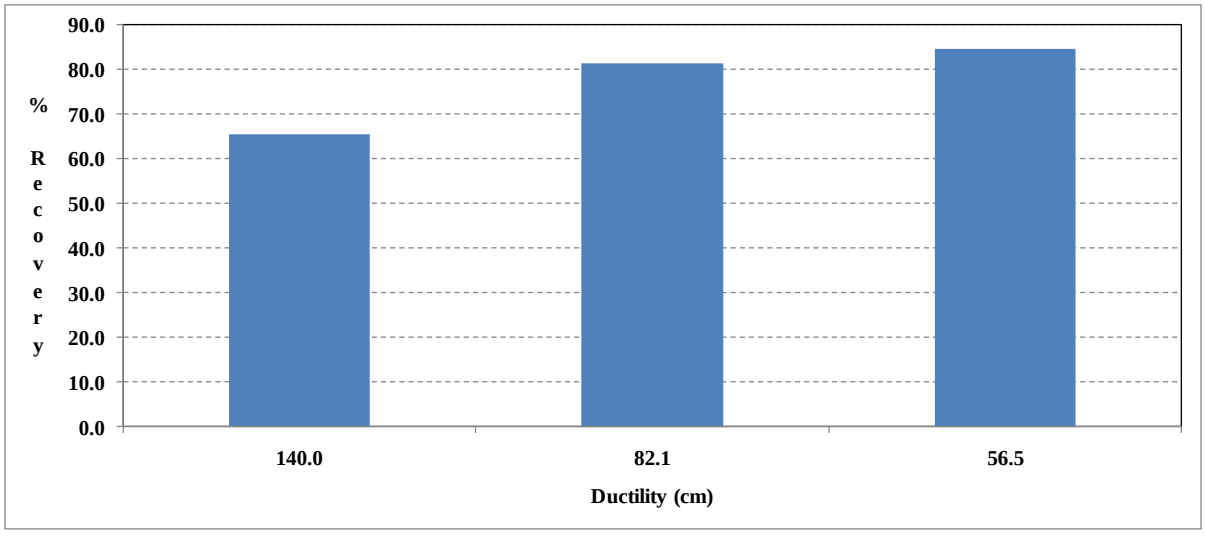


**(a)**

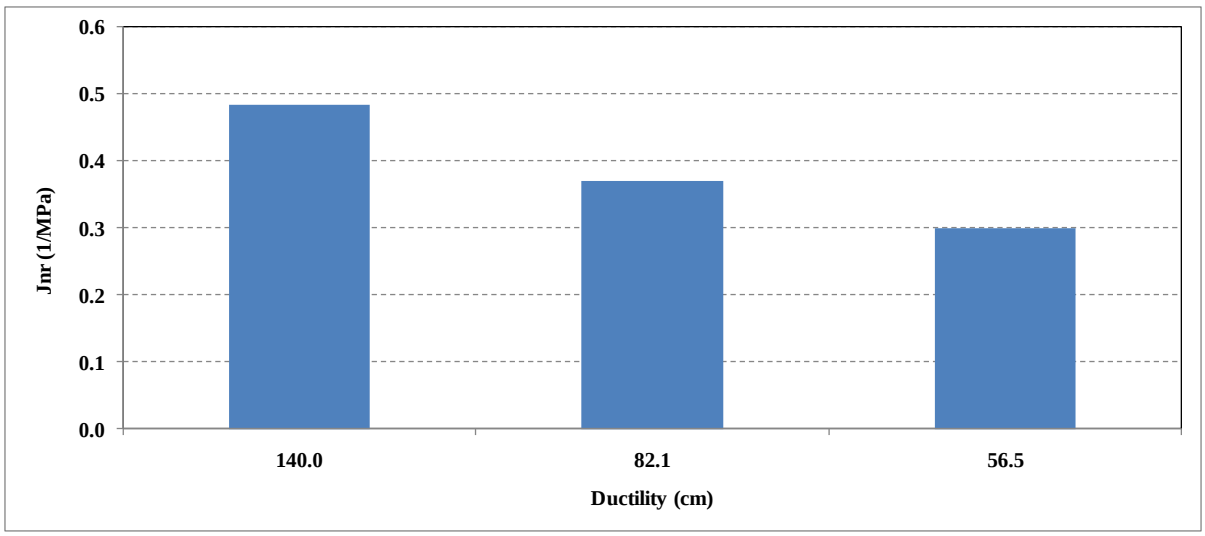


**(b)**

**Figure 33**
**Relationship between the binder ductility and (a) percentage recovery and (b) non-recoverable creep compliance**

# SUMMARY AND CONCLUSIONS

Instrument responses in past ALF experiments were analyzed to quantify the variation of pavement responses with temperature and its relationship to pavement performance. Measurements were also used to determine the effectiveness of stress and strain measurements in past experiments and the use of sensor technology to monitor pavement damage. Results of this analysis were used to suggest possible modifications to the instrumentation strategy in the upcoming ALF Experiment V.

Analysis conducted in this study established the relationship between the binder deformation properties at intermediate and low temperature and mix performance. Nine straight binders obtained from two major asphalt suppliers were tested using the ductility test, the direct tensile test, and the multiple stress creep recovery test. All selected binders were classified as PG 64-22 according to the Superpave binder specification system. To assess the results of these tests, selected asphalt binders were evaluated using high pressure gel permeation chromatography, differential scanning calorimetry, and dynamic mechanical analysis. In addition, three binders with contrasting levels of ductility were used to prepare asphalt mixes, which were evaluated using the ITS test.

## Analysis of ALF Instrument Responses

Based on the results of this analysis, the following conclusions may be drawn:

- Repeatability of stress and strain measurements was acceptable in most cases. Repeatability of pavement responses was better in Experiment III than Experiment II. Responses in Experiment II were somewhat lower in magnitude than in Experiment III, which may have resulted in greater variability in the responses.
- Survivability of the gages was deemed acceptable. However, installed pressure cells in the granular layers appeared to tilt during construction or after the loading started possibly due to poor compaction of the supportive layer. With the increase in the number of passes, signals became noisier, but the peak response could still easily be extracted.
- Pavement responses were strongly influenced by the temperature during testing. An exponential model provided acceptable description of this variation.
- Strain gages were not a reliable indicator of damage development in HMA. It appears that with the increase in the number of passes, the strain gages disperse the material around them resulting in less contact with the surrounding medium and therefore, a smaller strain was measured.

- Measured vertical stress remained fairly constant with the increase in the number of passes. This observation indicates that the stress applied on the material mainly depends on the magnitude of the external load and not on the level of damage in the material.
- Based on the analysis conducted in this study, a number of modifications to past instrumentation strategies are recommended and were discussed in the analysis section.

**Evaluation of Ductility Specifications**

Based on the results of laboratory testing conducted in this study, it can be concluded that the measurement of binder ductility is beneficial to the state and correlates well with mix performance at intermediate temperature. This test may not be substituted with the direct tensile test or the multiple stress creep recovery test. In addition, the following conclusions may be drawn:

- An inverse correlation was found between binder ductility at 25$^{o}$C and the measured failure strain at -12$^{o}$C. In other words, a binder that provides high ductility at intermediate temperature would be characterized by poor elongation properties at low temperature. This behavior was linked to the binder chemical compositions, which revealed the following:
    - An increase in the binder content of LMW results in an increase in its ductility at intermediate temperature.
    - An increase in the binder content of crystallizable LMW results in crystallization of these molecular fractions at low temperature. Due to their crystalline nature, these components are characterized by brittle and stiff physical behavior at low temperatures. In addition, an increase in maltene content results in some of the light components to crystallize at higher temperature as it approaches the glassy region.
- All tested binders lost part of their low molecular weight content during aging resulting in an increase in the asphaltene content in the aged binder. Binders with the same crude oil source lost about 2% of their low molecular weight components in the aging process.
- Performance of the binder can be strongly linked to its chemical constituents. A positive correlation exists between the percentage of LMW in the binder and its rutting resistance as predicted by the criterion of G*/sinδ for the original binder. In contrast, the increase in LMW results in an increase in the binder stiffness at low temperatures.
- Current Superpave specifications failed to differentiate between these binders in terms of performance since they may all be used as PG 64-22 binders and are expected to exhibit similar pavement performance. Since past research has widely established the relationship

between asphalt ductility and pavement performance, it would be expected that these binders would not exhibit the same performance in the field.

- There was a positive correlation between the binder ductility and the measured tensile strength of the mixture as well as its strain at failure. Using a binder with a high ductility resulted in a mixture with greater indirect tensile strength and a stronger ability to resist cracking at intermediate temperatures.
- An inverse correlation was found between binder ductility and percentage recovery in the MSCR test. Moreover, a binder with high ductility would be characterized by high non-recoverable creep compliance. This means that a binder characterized with a high level of ductility would exhibit poor performance in the MSCR test.

# RECOMMENDATIONS

As a result of the analysis conducted in this study, the following recommendations are offered to the Louisiana Department of Transportation and Development:

- Proposed modifications to the instrumentation strategy in Experiment V should be implemented. In addition, the use of cement-stabilized materials at the ALF facility needs to be investigated as the use of this pavement material extends the experiment over a long period of time that may not be necessary.
- Evaluation of fiber-optic strain gages in future experiments at the ALF facility should be conducted.
- The ductility test should be kept in the state binder's specifications as it correlates well with mix performance at intermediate temperatures. This test may not be substituted with the direct tensile test or the multiple stress creep recovery test.
- Additional laboratory testing should be conducted to relate the rheological properties of the binder at low temperatures with the mixture performance at low temperatures.

# ACRONYMS, ABBREVIATIONS, AND SYMBOLS

| | |
|---|---|
| ALF | accelerated loading facility |
| APT | accelerated pavement testing |
| AR | asphalt rubber |
| BBR | bending beam rheometer |
| DMA | dynamic mechanical analysis |
| DTT | direct tensile test |
| DSR | dynamic shear rheometer |
| DSC | differential scanning calorimetry |
| ESAL | equivalent single axle load |
| FHWA | Federal Highway Administration |
| ft. | foot |
| FWD | falling weight deflectometer |
| HMA | hot-mix asphalt |
| HP-GPC | high pressure gel permeation chromatography |
| in. | inch |
| ITS | indirect tensile strength |
| LADOTD | Louisiana Department of Transportation and Development |
| lb. | pound |
| LMW | light molecular weight |
| LTRC | Louisiana Transportation Research Center |
| LVDT | linear variable deformation transducer |
| min. | minute |
| MMW | medium molecular weight |
| MSCR | multiple-stress creep recovery |
| Pa | Pascal |
| PAV | pressure aging vessel |
| PG | performance grade |
| psi | pound per square inch |
| RAP | reclaimed asphalt pavement |
| RTFO | rolling thin film oven |
| SI | International System of Units |
| sec | second |
| VLMW | very low molecular weight |

# REFERENCES


1. White, T.D. “Instrumentation and Pavement Design,” *Symposium on the State-of-the-Art of Pavement Response Monitoring Systems for Roads and Airfields*, sponsored by U.S. Army Cold Regions Research and Engineering Laboratory, Report 89-23, 1989, pp. 2-8.

2. Ullidtz, P. *Pavement Analysis*, Elsevier Science, New York, NY, 1987.

3. Ullidtz, P. State-of-the-Art Stress, Strain and Deflection Measurements,” *Symposium on the State-of-the-Art of Pavement Response Monitoring Systems for Roads and Airfields*, sponsored by U.S. Army Cold Regions Research and Engineering Laboratory, Report 89-23, 1989, pp. 148-161.

4. Tabatabaee, N., and Sebaaly, P. State-of-the-Art Pavement Instrumentation. Transportation Research Record 1260, Transportation Research Board, Washington, D.C., 1990, pp. 246-255.

5. Huhtala, M.; Alkio, R.; Pihlajamaki, J.; Pienimaki, M.; and Halonen, P. “Behavior of Bituminous Materials under Moving Wheel Loads,” *Proceedings of the Annual Meeting of the Association of Asphalt Paving Technologists*, Vol. 65, Baltimore, MD, 1992, pp. 422-443.

6. Vogelzang, C.H., and Bouman, S.R. In-Situ Stress and Strain Measurements in Dynamically Loaded Asphalt Pavement Structures. Proceedings of Conference Sponsored by the U.S. Army Cold Regions Research and Engineering Laboratory - Road and Airport Pavement Response Monitoring Systems, Federal Aviation Administration, West Lebanon, New Hampshire, American Society of Civil Engineers, 1992, pp. 245-259.

7. Selig, E.T. In-Situ Stress Measurements. Symposium on the State-of-the-Art of Pavement Response Monitoring Systems for Roads and Airfields, sponsored by U.S. Army Cold Regions Research and Engineering Laboratory, Report 89-23, 1989, pp. 162-168.

8. Ullidtz, P. Modelling Flexible Pavement Response and Performance, 1st ed., Polyteknisk Forlag, Denmark, 1998.

9. Torry, A.C., and Sparrow, R.W. The Influence of the Diaphragm Flexibility on the Performance of an Earth Pressure Cell. Journal of Scientific Instruments, Vol. 44, 1967, pp. 781-785.

10. Ghuzlan, K.A., and Carpenter, S.H. Energy-Derived, Damage-Based Failure Criterion for Fatigue Testing. In *Transportation Research Record: 1723*, TRB, National Research Council, Washington, D.C., 2000, pp. 141-149.

11. Rodrigues, R.M. A Model for Fatigue Cracking Prediction of Asphalt Pavements Based on Mixture Bonding Energy. *International Journal of Pavement Engineering*, Vol. 1 (2), 2000, pp. 133-149.

12. Halstead, W.J. The Relation of Asphalt Ductility to Pavement Performance. Proc., Association of Asphalt Pavement Technologists, Vol. 32, 1963, pp. 247-270.

13. Kandhal, P.S., and Koehler, W.C. Effect of Rheological Properties of Asphalts on Pavement Cracking. Asphalt Theology: Relationship to Mixture, ASTM STP 941, O.E. Briscoe, Ed., American Society for Testing and Materials, Philadelphia, 1987, pp. 99-117.

14. Dongre, R.; D'Angelo, J; and McMahon, S. Development of SuperPave Direct Tension Test Device. *Transportation Research Record No. 1586*, Transportation Research Board, Washington, D.C., 1997, pp. 32-39.

15. Dongre, R.; Button, J.W.; Kluttz, R.Q.; and Anderson, D.A. Evaluation of Superpave Binder Specification with Performance of Polymer-Modified Asphalt Pavements. *Progress of Superpave (Superior Performing Asphalt Pavement): Evaluation and Implementation*, ASTM STP 1322, R.N. Jester, Ed., American Society for Testing and Materials, 1997.

16. Yapp, M.T.; Durrani, A.Z.; and Finn, F.N. HP-GPC and Asphalt Characterization – Literature Review. Report No. SHRP-A/UIR-91-503, Strategic Highway Research Program, National Research Council, Washington, D.C., 1991.

17. Shen, J.; Amirkhanian, S.; and Xiao, F. High-Pressure Gel Permeation Chromatography of Aging of Recycled Crumb Rubber-Modified Binders with Rejuvenating Agents. Transportation Research Record: Journal of the Transportation Research Board, No. 1962, National Research Council, Washington, D.C., 2006, pp. 21-27.

18. Negulescu, I.I., and Daly, W.H. Application of Oscillating DSC to the Detection of Thermal Transitions in Poly (γ-Alkyl-γ, L-Glutamates), *Polymer Preprints*, Vol. 35(1), 1994, pp. 441-442.

19. Lytton, R.L.; Masad, E.A.; Zollinger, C.; Bulut, R.; and Little, D. Measurements of Surface Energy and Its Relationship to Moisture Damage. Report No. FHWA/TX-05/0-4524-2, College Station, TX, 2005.

20. Asphalt Institute, Performance Graded Asphalt Binder Specification and Testing - I: Background, SuperPave™ Series no.1 (SP-1), 1997.

21. Roberts, F.L.; Kandhal, P.S.; Brown, E.R.; Lee, D.; and Kennedy, T.W. Hot Mix Asphalt Materials, Mixture Design, and Construction. 2nd Edition, Napa Education Foundation, Lanham, MD, 1996.

22. King, W.M., and Abadie. C. Comparative Performance of Conventional and Rubberized Hot Mix under Accelerated Loading – Construction Report. FHWA/LA-99/331, Louisiana Transportation Research Center, Louisiana Department of Transportation, Baton Rouge, LA, 1999.

23. King, W.M. Evaluation of Stone/RAP Interlayers under Accelerated Loading – Construction Report. FHWA/LA-352, Louisiana Transportation Research Center, Louisiana Department of Transportation, Baton Rouge, LA, 2001.

24. Mohammad, L.N.; Rasoulian, M.; King, W.M.; Martinez; M., and Qi, Y. Evaluation of Stone/RAP Interlayers under Accelerated Loading. Report No. FHWA/LA.06/409, Louisiana Transportation Research Center, Louisiana Department of Transportation, Baton Rouge, LA, 2007.

25. Hugo, F. APT Performance Evaluation Using Seismic Wave Propagation and FDOT Report on Instrumentation. Available at The Heavy Vehicle Simulator (HVS) web site, http://www.gautrans-hvs.co.za/.

26. Roberts, F.L; Mohammad, L.N.; Qin, H.; and Huang, B. Comparative Performance of Rubber Modified Hot Mix Asphalt under ALF Loading. Report No. FHWA/LA.03/374, Louisiana Transportation Research Center, Baton Rouge, LA, 2003.

27. Mohammad, L.N.; Nazzal, M.; and Austin, A. Evaluation of Low Cost Asphalt Treated Base Mixtures. Presentation made at the Southeastern Asphalt/User Producer Group, San Antonio, TX, 2007.

28. AASHTO T314-07. Standard Method of Test for Determining the Fracture Properties of Asphalt Binder in Direct Tension (DT). Standard Specifications for Transportation Materials and Methods of Sampling and Testing, 25th Edition, 2007.

29. D'Angelo, J.; Kluttz, R.; Dongre, R.; Stephens, K.; and Zanzotto, L. Revision of the Superpave High Temperature Binder Specification: The Multiple Stress Creep Recovery Test. Journal of the Association of Asphalt Pavement Technologists, Vol. 76, 2007, pp. 123-162.

30. Al-Qadi, I.L.; Loulizi, A; Elseifi, M.A.; and Lahouar, S. The Virginia Smart Road: The Impact of Pavement Instrumentation on Understanding Pavement Performance. Journal of the Association of Asphalt Pavement Technologists, Vol. 73, 2004, pp. 427-465.

31. Huhtala, M., and Pihlajamaki, J. Strain and Stress Measurements in Pavements. Proceedings of Conference Sponsored by the U.S. Army Cold Regions Research and Engineering Laboratory - Road and Airport Pavement Response Monitoring Systems, Federal Aviation Administration, West Lebanon, New Hampshire, American Society of Civil Engineers, 1992, pp. 229-243.

32. Roque, R.; Guarin, A.; Wang, G.; Zou, J; and Mork, H. Develop Methodologies/Protocols to Assess Cracking Potential of Asphalt Mixtures Using Accelerated Pavement Testing. Final Report, Florida Department of Transportation, Tallahassee, FL, 2007.

33. Galal, K.; Sharp, S.R.; and Elfino, M.K. Fiber-Optic Sensors Strain Measurements under an Asphalt Layer during and after Construction. Paper No. 07-1712 Presented at the 86th Annual Transportation Research Board Annual Meeting, Transportation Research Board, Washington, D.C., 2007.

34. Sharp, S.R.; Cooper, K.R.; Clemena, G.G.; and Elfino, M.K. Fiber-Optic Based Strain Sensor for Asphalt Pavement. Paper Presented at the 84th Annual Transportation Research Board Annual Meeting, Transportation Research Board, Washington, D.C., 2005.

35. Shen, J.; Amirkhanian, S.; and Xiao, F. High-Pressure Gel Permeation Chromatography of Aging of Recycled Crumb Rubber-Modified Binders with Rejuvenating Agents. Transportation Research Record: Journal of the Transportation Research Board, No. 1962, National Research Council, Washington, D.C., 2006, pp. 21-27.